

Moment methods and realizable numerical methods for polydisperse sprays and particle-laden flows

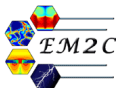
Marc Massot

Laboratory EM2C - UPR CNRS 288 - Ecole Centrale Paris
Fédération de Mathématiques de l'Ecole Centrale Paris - FR CNRS 3487

In collaboration with

A. Larat, M. Boileau, F. Laurent (CNRS - EM2C - ECP - Fédé ECP)
C. Chalons (UVSQ - Fédé ECP),
R. O. Fox (Iowa State University - EM2C - ECP - Fédé ECP),
A. Vié (Stanford - Center for Turbulence Research - EM2C - ECP)

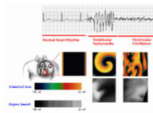
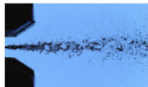
Workshop on Moment Methods in Kinetic Theory II - Fields Institute - Toronto



A mathematics team in an engineering laboratory

➤ Four fields of applications :

- Flame Dynamics, homogeneous and two-phase **combustion**
- Multi-scale reaction fronts in **Nonlinear chemical dynamics and biomedical engineering** (spiral and scroll waves, strokes, ...)
- **Atmospheric pressure discharges** (Streamers) for flame stabilization and out of thermal and chemical equilibrium weakly ionized plasma flows for **atmospheric re-entry**
- Separated and disperse two-phase flows, polydisperse spray flows for **combustion chambers in automotive, aeronautic and solid propulsion applications.**



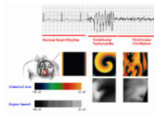
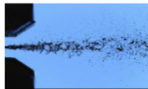
Mathematics fields of research (EDP, Numerical Analysis, HPC)

- Moment methods for kinetic equations describing disperse two-phase flows, realizable high order numerical methods and asymptotic limits (border of the moment space)
- Adaptation in time and space, with error control based on operator splitting methods and multiresolution analysis for the propagation of stiff reaction fronts
- Derivation of thermodynamically consistent and well-posed fluid models for weakly ionized plasma flows out of thermal and chemical equilibrium using kinetic theory

A mathematics team in an engineering laboratory

➤ Four fields of applications :

- Flame Dynamics, homogeneous and two-phase **combustion**
- Multi-scale reaction fronts in **Nonlinear chemical dynamics and biomedical engineering** (spiral and scroll waves, strokes, ...)
- **Atmospheric pressure discharges** (Streamers) for flame stabilization and out of thermal and chemical equilibrium weakly ionized plasma flows for **atmospheric re-entry**
- Separated and disperse two-phase flows, polydisperse spray flows for **combustion chambers in automotive, aeronautic and solid propulsion applications.**

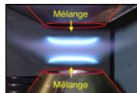


Mathematics fields of research (EDP, Numerical Analysis, HPC)

- **Moment methods for kinetic equations describing disperse two-phase flows, realizable high order numerical methods and asymptotic limits (border of the moment space)**
- **Adaptation in time and space, with error control based on operator splitting methods and multiresolution analysis for the propagation of stiff reaction fronts**
- **Derivation of thermodynamically consistent and well-posed fluid models for weakly ionized plasma flows out of thermal and chemical equilibrium using kinetic theory**

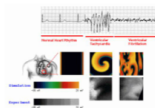
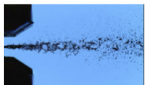
A mathematics team in an engineering laboratory

- Part of the “Fédération de Mathématiques de l’Ecole Centrale Paris”
- Membre associé de la Fondation Mathématique Jacques Hadamard, Université Paris-Saclay



Fondation mathématique
FMJH
Jacques Hadamard

Campus Paris Saclay
FONDATION DE COOPERATION SCIENTIFIQUE



Context

Industrial applications

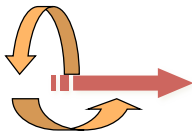
- Liquid propulsion: aeronautic or automotive combustion chambers,
- Solid propulsion: solid rocket motor (alumina droplets),

Liquid injection



Source: C. Dumouchel CORIA Rouen

Evaporation + Partial mixing



Swirl of oxydant

Combustion



Source: Pr Edwards, Stanford

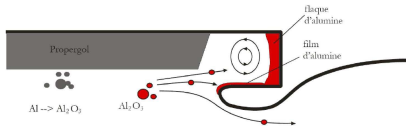
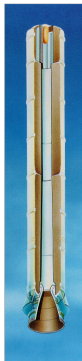
Combustion of polydisperse evaporating sprays

- Atomization of the liquid phase
- Mixing of the fuel and the air in the vapor phase
- Combustion regimes and dynamics

Context

Industrial applications

- Liquid propulsion: aeronautic or automotive combustion chambers,
- Solid propulsion: solid rocket motor (alumina droplets),



Propellant is aluminized to increase specific impulse \Rightarrow droplets of liquid aluminum oxide

Context

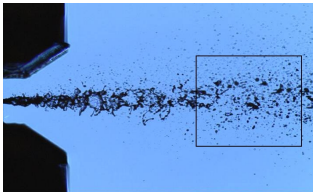
Industrial applications

- Liquid propulsion: aeronautic or automotive combustion chambers,
- Solid propulsion: solid rocket motor (alumina droplets),

Presence of a disperse liquid phase: droplets with a large size spectrum

- **Droplets-gaz interactions**
drag force, evaporation, heat transfer
- **Droplets-droplets interactions**
collision, breakup

Key parameter: droplet size



- Neglected volume fraction (source term for gaz equations)
- The flow around the droplets is not resolved
- Spherical droplets

Modelization of the disperse phase

Kinetic model

$f(\mathbf{x}, \mathbf{u}, S, T; t)$: number density function (NDF)

Transport equation of Boltzmann type [Williams 1958],

$$\underbrace{\partial_t f + \partial_{\mathbf{x}} \cdot (\mathbf{u} f)}_{\text{free transport}} - \underbrace{\partial_S(Kf)}_{\text{evaporation}} + \underbrace{\partial_{\mathbf{u}}(\mathbf{F} f)}_{\text{forces}} + \underbrace{\partial_T(E f)}_{\text{heat exchanges}} = \underbrace{\Gamma(f, f)}_{\text{collisions}} + \underbrace{Q(f)}_{\text{breakup}}$$

- evaporation and heating : d^2 law ($K = \text{cste}$, $E = 0$), infinite conductivity, ...

- drag and gravity : $F = \frac{\mathbf{u}_g - \mathbf{u}}{\tau_p} \left(1 + \frac{\text{Re}^{2/3}}{6}\right) + g$

- coalescence : $\Gamma(f, f) = - \int_{S^*} \int_{\mathbf{u}^*} f f^* \beta(S, S^*) |\mathbf{u} - \mathbf{u}^*| dS^* d\mathbf{u}^*$
 $+ \frac{1}{2} \int_{S^* \in [0, S]} \int_{\mathbf{u}^*} f^\diamond f^* \beta(S^\diamond, S^*) |\mathbf{u}^\diamond - \mathbf{u}^*| J dS^* d\mathbf{u}^*$

- rebounds : $\Gamma(f, f) = \int_{\mathbb{R}} \beta(S, S^*) \int_{\mathbb{R}^d} \int_{S^+} [f' f'^* - f f^*] |(\mathbf{u} - \mathbf{u}^*) \cdot \mathbf{n}| d\mathbf{n} d\mathbf{u}^* dS^*$

- secondary breakup PhD [Dufour, 2005, Doisneau, 2013]

Modelization of the disperse phase

Kinetic model

$f(\mathbf{x}, \mathbf{u}, S, T; t)$: number density function (NDF)

Transport equation of Boltzmann type [Williams 1958],

$$\underbrace{\partial_t f + \partial_{\mathbf{x}} \cdot (\mathbf{u} f)}_{\text{free transport}} - \underbrace{\partial_S(Kf)}_{\text{evaporation}} + \underbrace{\partial_{\mathbf{u}}(\mathbf{F} f)}_{\text{forces}} + \underbrace{\partial_T(E f)}_{\text{heat exchanges}} = \underbrace{\Gamma(f, f)}_{\text{collisions}} + \underbrace{Q(f)}_{\text{breakup}}$$

Lagrangian description

particular discretization - Monte-Carlo methods

[O'Rourke, 1981, Dukowicz, 1980, Bird, 1994]

advantages

- usable in most cases
- no numerical diffusion

disadvantages

- slow convergence
- difficulties for parallelization
- coupling with the Eulerian description of the gas



Modelization of the disperse phase

Kinetic model

$f(\mathbf{x}, \mathbf{u}, S, T; t)$: number density function (NDF)

Transport equation of Boltzmann type [Williams 1958],

$$\underbrace{\partial_t f + \partial_{\mathbf{x}} \cdot (\mathbf{u} f)}_{\text{free transport}} - \underbrace{\partial_S (Kf)}_{\text{evaporation}} + \underbrace{\partial_{\mathbf{u}} (\mathbf{F} f)}_{\text{forces}} + \underbrace{\partial_T (E f)}_{\text{heat exchanges}} = \underbrace{\Gamma(f, f)}_{\text{collisions}} + \underbrace{Q(f)}_{\text{breakup}}$$

Eulerian description

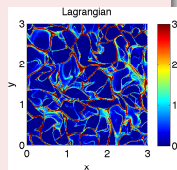
- Moments of the NDF: $M_{i,j,k}(t, \mathbf{x}) = \int \int S^i \mathbf{u}^j T^k f(\mathbf{x}, \mathbf{u}, S, T; t) dT d\mathbf{u} dS$
- System of conservation equations on moments

advantages

- more easy to parallelize
- natural coupling with the Eulerian description of the gas

disadvantages

- model (closures)
- adapted numerical schemes (hypercompressibility, vacuum zones)



Modelization of the disperse phase: a simplified case

Simplified and dimensionless kinetic model

$f(\mathbf{x}, \mathbf{u}, S, \mathcal{T}; t)$: number density function (NDF)

Transport equation of Boltzmann type [Williams 1958],

$$\underbrace{\partial_t f + \partial_{\mathbf{x}} \cdot (f \mathbf{u})}_{\text{free transport}} - \underbrace{\partial_S (Kf)}_{\text{evaporation}} + \underbrace{\partial_{\mathbf{u}} \left(\frac{\mathbf{U}_g - \mathbf{u}}{\text{St}(S)} f \right)}_{\text{Stokes drag}} + \underbrace{\partial_T (E f)}_{\text{heat exchanges}} = \underbrace{\Gamma(f, f)}_{\text{collisions}} + \underbrace{Q(f)}_{\text{breakup}}$$

Eulerian description

- Moments of the NDF: $M_{i,j,k} = \int \int S^i \mathbf{u}^j \mathcal{T}^k f(\mathbf{x}, \mathbf{u}, S, \mathcal{T}; t) d\mathcal{T} d\mathbf{u} dS$
- System of conservation equations on moments

$$S \in [0, 1]$$

$$\mathbf{u} \in \mathbb{R}^d$$

Modelization of the disperse phase: a simplified case

Simplified and dimensionless kinetic model

$f(\mathbf{x}, \mathbf{u}, S; t)$: number density function (NDF)

Transport equation of Boltzmann type [Williams 1958],

$$\underbrace{\partial_t f + \partial_{\mathbf{x}} \cdot (f \mathbf{u})}_{\text{free transport}} - \underbrace{\partial_S(Kf)}_{\text{evaporation}} + \underbrace{\partial_{\mathbf{u}} \left(\frac{\mathbf{U}_g - \mathbf{u}}{\text{St}(S)} f \right)}_{\text{Stokes drag}} = 0$$

Eulerian description

- Moments of the NDF: $M_i^j = \int \int S^i \mathbf{u}^j f(\mathbf{x}, \mathbf{u}, S; t) d\mathbf{u} dS$
- System of conservation equations on moments

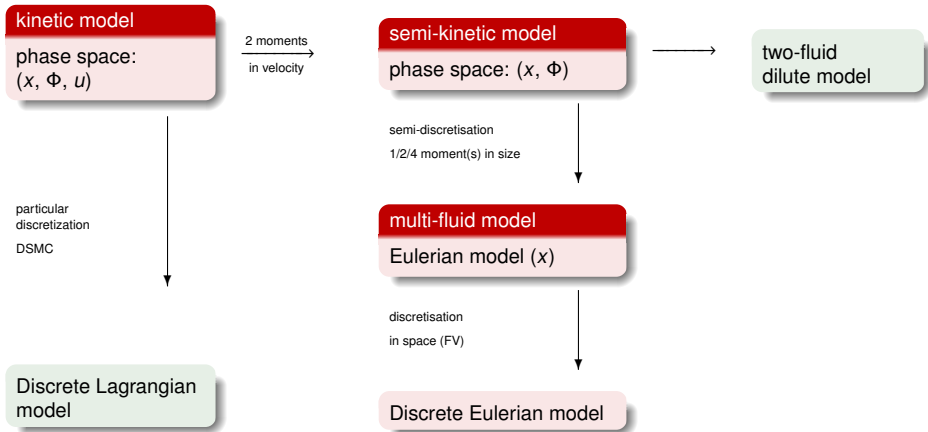
$$S \in [0, 1]$$

$$\mathbf{u} \in \mathbb{R}^d$$

Discretization Strategies for Polydisperse sprays

Size polydispersion and evolution has been successfully handled

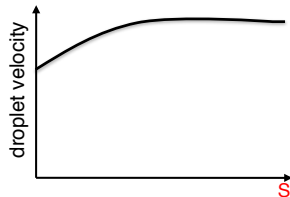
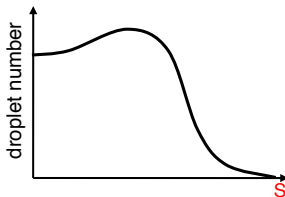
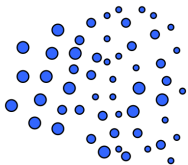
PhD de Chaisemartin 2009, Fréret et al 2009, 2010, 2012, Kah, 2010 (SMAI/GAMNI - ECCOMAS), Doisneau 2013, Massot et al. SIAP 2010, Kah et al. JCP 2012, Vié et al. JCP 2013, Doisneau et al. JCP 2013, Doisneau et al. JPP 2014



Eulerian multi-fluid models

Principle of the method (simplified case)

A conservation law system for each size interval (section)



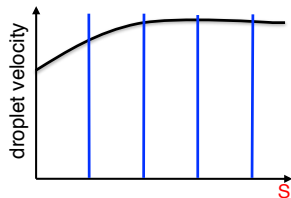
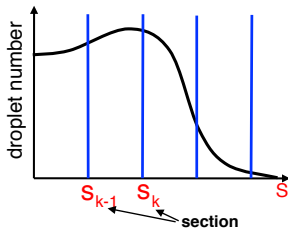
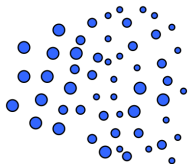
Assumptions :

$$f(t, \mathbf{x}, \mathbf{u}, S) = n(t, \mathbf{x}, S)\delta(\mathbf{u} - \mathbf{u}_d(t, \mathbf{x}, S))$$

Eulerian multi-fluid models

Principle of the method (simplified case)

A conservation law system for each size interval (section)



Considered moments:

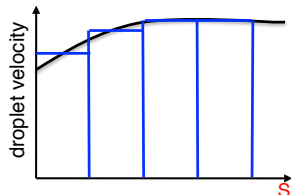
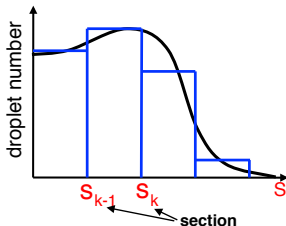
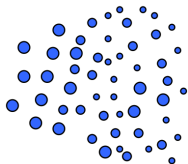
$$m^{(j)}(t, \mathbf{x}) = \int_{S_{j-1}}^{S_j} S^{3/2} \int f(t, \mathbf{x}, \mathbf{u}, S) d\mathbf{u} dS$$

$$m^{(j)} u^{(j)}(t, \mathbf{x}) = \int_{S_{j-1}}^{S_j} S^{3/2} \int \mathbf{u} f(t, \mathbf{x}, \mathbf{u}, S) d\mathbf{u} dS$$

Eulerian multi-fluid models

Principle of the method (simplified case)

A conservation law system for each size interval (section)



presumed pdf in each section k

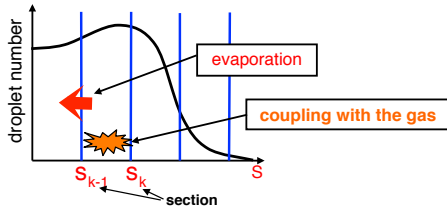
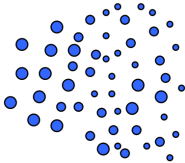
$$n(t, \mathbf{x}, S) = m^{(k)}(t, \mathbf{x}) \kappa^{(k)}(S)$$

$$\mathbf{u}_d(t, \mathbf{x}, S) = \mathbf{u}_d^{(k)}(t, \mathbf{x})$$

Eulerian multi-fluid models

Principle of the method (simplified case)

A conservation law system for each size interval (section)



Equations: [Laurent and Massot, 2001]

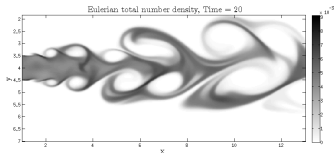
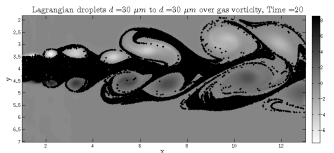
$$\partial_t(m^{(k)}) + \partial_x \cdot (m^{(k)} u^{(k)}) = -(E_1^{(k)} + E_2^{(k)})m^{(k)} + E_1^{(k+1)}m^{(k+1)}$$

$$\partial_t(m^{(k)} u^{(k)}) + \partial_x \cdot (m^{(k)} u^{(k)} \otimes u^{(k)}) = -(E_1^{(k)} + E_2^{(k)})m^{(k)} u^{(k)} + E_1^{(k+1)}m^{(k+1)} u^{(k+1)} \\ + m^{(k)} F^{(k)}$$

Eulerian multi-fluid models

Eulerian multi-fluid models

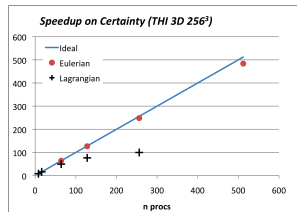
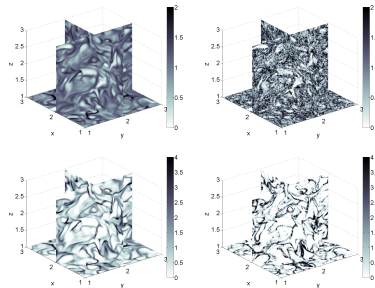
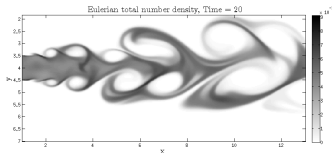
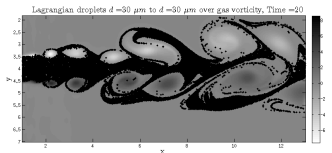
- Very good agreement with the Lagrangian model [de Chaisemartin, 2009]
- Validation through comparisons with experiments [Freret et al., 2008]
- Efficient parallelization [Freret et al., 2010]



Eulerian multi-fluid models

Eulerian multi-fluid models

- Very good agreement with the Lagrangian model [de Chaisemartin, 2009]
- Validation through comparisons with experiments [Freret et al., 2008]
- Efficient parallelization [Fr eret et al., 2010]

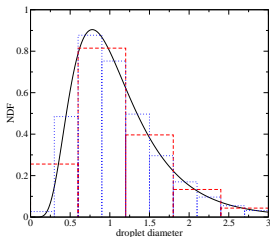


Eulerian multi-fluid model

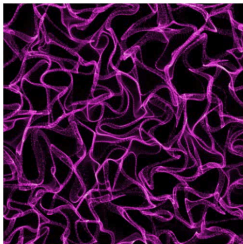
Code MUSES3D - S. de Chaisemartin, L. Fréret

Conservation equations for each size interval:

$$\begin{aligned}\partial_t m^{(j)} + \partial_x \cdot (m^{(j)} u_d^{(j)}) &= 0 \\ \partial_t (m^{(j)} u_d^{(j)}) + \partial_x \cdot (m^{(j)} u_d^{(j)} \otimes u_d^{(j)}) &= m^{(j)} F^{(j)}\end{aligned}$$

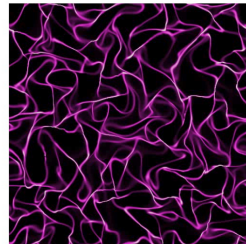


Lagrangian



Asphodele code (CORIA - CNRS URM 6614)
Muses3d code (EM2C - CNRS ECP)

Eulerian



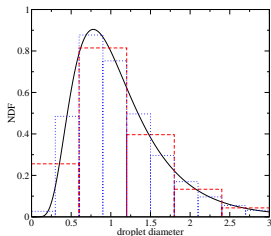
Thomine, Freret, Reveillon & Massot

Eulerian multi-fluid model

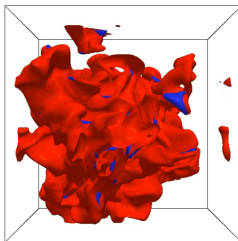
Code MUSES3D - S. de Chaisemartin, L. Fréret

Conservation equations for each size interval:

$$\begin{aligned}\partial_t m^{(j)} + \partial_{x_i} (m^{(j)} u_d^{(j)}) &= 0 \\ \partial_t (m^{(j)} u_d^{(j)}) + \partial_{x_i} (m^{(j)} u_d^{(j)} \otimes u_d^{(j)}) &= m^{(j)} F^{(j)}\end{aligned}$$

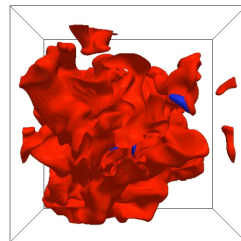


Lagrangian



Asphodele code (CORIA - CNRS UMR 6614)
Mused code (EMC - CNRS ECP)

Eulerian



Thomine, Freret, Revellon & Massot

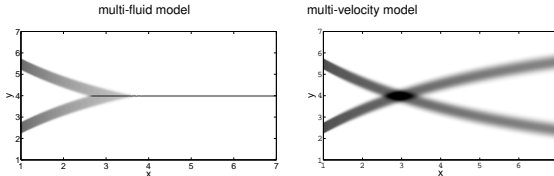
Eulerian multi-fluid model

Code MUSES3D - S. de Chaisemartin, L. Fréret

Conservation equations for each size interval:

$$\begin{aligned}\partial_t m^{(j)} + \partial_x \cdot (m^{(j)} u_d^{(j)}) &= 0 \\ \partial_t (m^{(j)} u_d^{(j)}) + \partial_x \cdot (m^{(j)} u_d^{(j)} \otimes u_d^{(j)}) &= m^{(j)} F^{(j)}\end{aligned}$$

- mono-kinetic assumption at a given size, location and time
Equivalent to pressureless gas dynamics
For DNS and Low Stokes numbers



Key issue : accurate schemes in space and time

Eulerian multi-fluid model

Code MUSES3D - S. de Chaisemartin, L. Fréret

Conservation equations for each size interval:

$$\begin{aligned}\partial_t m^{(j)} + \partial_x \cdot (m^{(j)} u_d^{(j)}) &= 0 \\ \partial_t (m^{(j)} u_d^{(j)}) + \partial_x \cdot (m^{(j)} u_d^{(j)} \otimes u_d^{(j)}) &= m^{(j)} F^{(j)}\end{aligned}$$

- one-moment per section leads to a first order moment method
strong numerical diffusion in size phase space
several sections needed for an accurate resolution of evaporation

Eulerian multi-fluid model

Code MUSES3D - S. de Chaisemartin, L. Fréret

Conservation equations for each size interval:

$$\begin{aligned}\partial_t m^{(j)} + \partial_x \cdot (m^{(j)} u_d^{(j)}) &= 0 \\ \partial_t (m^{(j)} u_d^{(j)}) + \partial_x \cdot (m^{(j)} u_d^{(j)} \otimes u_d^{(j)}) &= m^{(j)} F^{(j)}\end{aligned}$$

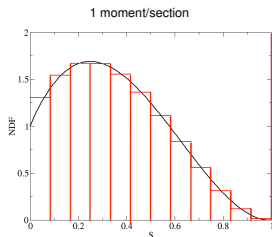
- one-moment per section leads to a first order moment method
strong numerical diffusion in size phase space
several sections needed for an accurate resolution of evaporation

**General objectif : design higher order moment methods in size and velocity
which preserve realizability
and built-in realizability preserving numerical methods - high order**

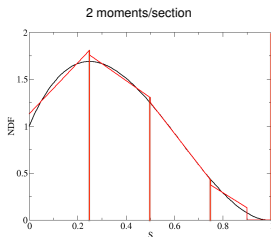
Outline

- 1 High order moment methods in size, with realizable and accurate numerical methods
- 2 High order moment methods in velocity, with realizable and accurate numerical methods
 - Up to second order moment methods (statistical crossing)
 - Higher order moment methods (deterministic crossing)
 - Multi-Gaussian model
- 3 Dealing with model coupling and asymptotic limits
 - A Hybrid model and related relaxation scheme
 - An Asymptotic-Preserving Relaxation scheme

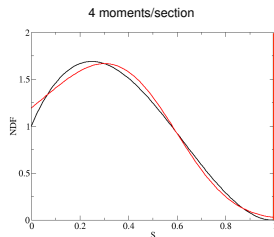
Evolution of the Eulerian multi-fluid models



[Laurent and Massot, 2001]

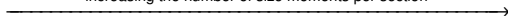


[Laurent, 2006, Doisneau et al 2013]

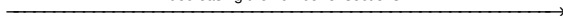


[Massot et al., 2010, Kah et al 2012]

increasing the number of size moments per section



decreasing the number of sections

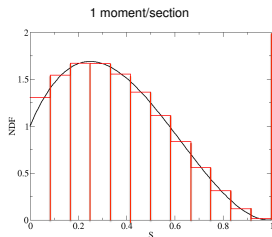


decreasing the cost

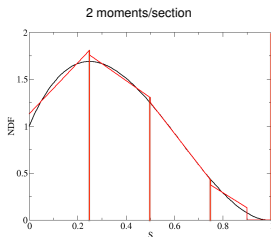
increasing the model complexity



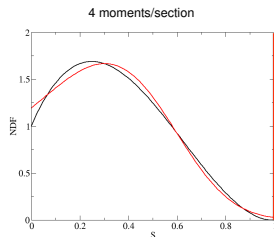
Evolution of the Eulerian multi-fluid models



[Laurent and Massot, 2001]

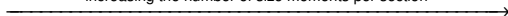


[Laurent, 2006, Doisneau et al 2013]



[Massot et al., 2010, Kah et al 2012]

increasing the number of size moments per section



decreasing the number of sections



decreasing the cost

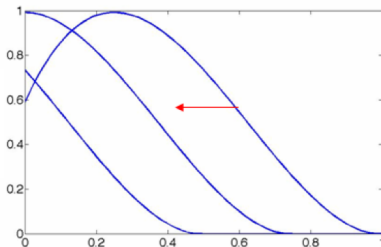
increasing the model complexity



Moment method for purely evaporating case

Kinetic model for purely evaporating case, d^2 law, dimensionless

$$\begin{cases} \partial_t f - \partial_S(K f) = 0, & t \in \mathbb{R}^+, S \geq 0 \\ f(0, S) = f_0(S), & S \geq 0 \end{cases}$$

with $K = \mathbb{K}_{[0, +\infty[}(S)$ solution: $f(t, S) = \left(\int_0^t f_0(\sigma) d\sigma \right) \delta_0(S) + f_0(S + t)$ Moments: $\mathcal{M}_k = \int_0^1 S^k f(S) dS, k = 0, \dots, N$

System to solve:

$$d_t \mathcal{M} = -A \mathcal{M} - \phi_-, \quad \mathcal{M} = (\mathcal{M}_0, \dots, \mathcal{M}_N)^t$$

Moment method for purely evaporating case

Kinetic model for purely evaporating case, d^2 law, dimensionless

$$\begin{cases} \partial_t f - \partial_S(f) = 0, & t \in \mathbb{R}^+, S \geq 0 \\ f(0, S) = f_0(S), & S \geq 0 \end{cases}$$

Moments: $\mathcal{M}_k = \int_0^1 S^k f(S) dS, k = 0, \dots, N$

System to solve:

$$d_t \mathcal{M} = -A \mathcal{M} - \phi_-, \quad \mathcal{M} = (\mathcal{M}_0, \dots, \mathcal{M}_N)^t$$

with

$$\phi_- = f(t, 0) \begin{pmatrix} 1 \\ 0 \\ \vdots \\ 0 \end{pmatrix}, \quad A = \begin{bmatrix} 0 & & & & & \mathbf{0} \\ 1 & 0 & & & & \\ & 2 & \ddots & & & \\ & & \ddots & \ddots & & \\ \mathbf{0} & & & & N & 0 \end{bmatrix}.$$

- **closure problem:** pointwise values of f from its moments
- **realizability problem:** \mathcal{M} has to stay in the moment space

Moment method for purely evaporating case

Kinetic model for purely evaporating case, d^2 law, dimensionless

$$\begin{cases} \partial_t f - \partial_S(f) = 0, & t \in \mathbb{R}^+, S \geq 0 \\ f(0, S) = f_0(S), & S \geq 0 \end{cases}$$

Moments: $\mathcal{M}_k = \int_0^1 S^k f(S) dS, k = 0, \dots, N$

System to solve:

$$d_t \mathcal{M} = -A \mathcal{M} - \phi_-, \quad \mathcal{M} = (\mathcal{M}_0, \dots, \mathcal{M}_N)^t$$

with

$$\phi_- = f(t, 0) \begin{pmatrix} 1 \\ 0 \\ \vdots \\ 0 \end{pmatrix}, \quad A = \begin{bmatrix} 0 & & & & & \mathbf{0} \\ 1 & 0 & & & & \\ & 2 & \ddots & & & \\ & & \ddots & \ddots & & \\ \mathbf{0} & & & & N & 0 \end{bmatrix}.$$

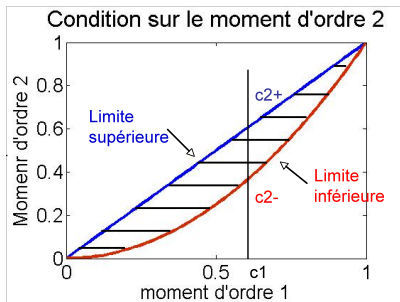
- **closure problem**: pointwise values of f from its moments
- **realizability problem**: \mathcal{M} has to stay in the moment space

Moment space

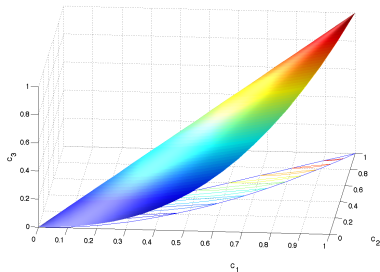
 N^{th} moment space of probability measures on $[0, 1]$

$$\widetilde{\mathcal{M}}_N = \{\mathbf{c}_N(\mu) | \mu \in \mathcal{P}\}, \quad \mathbf{c}_N(\mu) = (c_1(\mu), \dots, c_N(\mu))^t, \quad c_k(\mu) = \int_0^1 x^k d\mu(x).$$

→ convex space but “complex” geometry



$$c_1^2 < c_2 < c_1$$



$$\widetilde{\mathcal{M}}_3$$

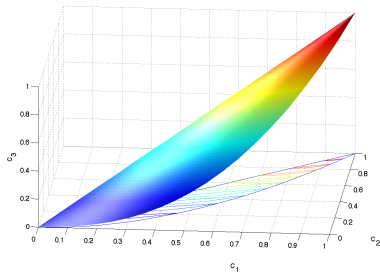
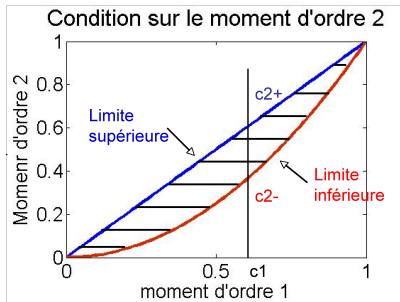
⇒ the numerical methods have to preserve this space

Moment space

N^{th} moment space of probability measures on $[0, 1]$

$$\widetilde{\mathcal{M}}_N = \{\mathbf{c}_N(\mu) | \mu \in \mathcal{P}\}, \quad \mathbf{c}_N(\mu) = (c_1(\mu), \dots, c_N(\mu))^t, \quad c_k(\mu) = \int_0^1 x^k d\mu(x).$$

→ convex space but “complex” geometry



⇒ the numerical methods have to preserve this space

Moment space

 N^{th} moment space of probability measures on $[0, 1]$

$$\widetilde{\mathcal{M}}_N = \{\mathbf{c}_N(\mu) | \mu \in \mathcal{P}\}, \quad \mathbf{c}_N(\mu) = (c_1(\mu), \dots, c_N(\mu))^t, \quad c_k(\mu) = \int_0^1 x^k d\mu(x).$$

Hankel determinants:

$$\underline{H}_{2m+d} = \begin{vmatrix} c_d & \dots & c_{m+d} \\ \vdots & & \vdots \\ c_{m+d} & \dots & c_{2m+d} \end{vmatrix} \quad \overline{H}_{2m+d} = \begin{vmatrix} c_{1-d} - c_{2-d} & \dots & c_m - c_{m+1} \\ \vdots & \vdots & \vdots \\ c_m - c_{m+1} & \dots & c_{2m-1+d} - c_{2m+d} \end{vmatrix}$$

 $\mathcal{M} = (c_1, \dots, c_N) \in \widetilde{\mathcal{M}}_N \Leftrightarrow \underline{H}_i \geq 0 \text{ and } \overline{H}_i \geq 0 \text{ for } d = 0, 1 \text{ and } i = 0, \dots, N.$
 $\mathcal{M} = (c_1, \dots, c_N) \in \overset{\circ}{\widetilde{\mathcal{M}}}_N \Leftrightarrow \underline{H}_i > 0 \text{ and } \overline{H}_i > 0 \text{ for } d = 0, 1 \text{ and } i = 0, \dots, N.$

Canonical moments [Dette and Studden, 1997]:

$$\rho_1 = c_1, \quad \rho_2 = \frac{c_2 - c_1^2}{c_1(1 - c_1)}, \quad \rho_3 = \frac{(1 - c_1)(c_1 c_3 - c_2^2)}{(c_2 - c_1^2)(c_1 - c_2)}, \quad \dots$$

bijection between the interior of $\overset{\circ}{\widetilde{\mathcal{M}}}_N$ and $]0, 1[^N$

Moment space

 N^{th} moment space of probability measures on $[0, 1]$

$$\widetilde{\mathcal{M}}_N = \{\mathbf{c}_N(\mu) | \mu \in \mathcal{P}\}, \quad \mathbf{c}_N(\mu) = (c_1(\mu), \dots, c_N(\mu))^t, \quad c_k(\mu) = \int_0^1 x^k d\mu(x).$$

Hankel determinants:

$$\underline{H}_{2m+d} = \begin{vmatrix} c_d & \dots & c_{m+d} \\ \vdots & & \vdots \\ c_{m+d} & \dots & c_{2m+d} \end{vmatrix} \quad \overline{H}_{2m+d} = \begin{vmatrix} c_{1-d} - c_{2-d} & \dots & c_m - c_{m+1} \\ \vdots & \vdots & \vdots \\ c_m - c_{m+1} & \dots & c_{2m-1+d} - c_{2m+d} \end{vmatrix}$$

 $\mathcal{M} = (c_1, \dots, c_N) \in \widetilde{\mathcal{M}}_N \Leftrightarrow \underline{H}_i \geq 0 \text{ and } \overline{H}_i \geq 0 \text{ for } d = 0, 1 \text{ and } i = 0, \dots, N.$
 $\mathcal{M} = (c_1, \dots, c_N) \in \overset{\circ}{\mathcal{M}}_N \Leftrightarrow \underline{H}_i > 0 \text{ and } \overline{H}_i > 0 \text{ for } d = 0, 1 \text{ and } i = 0, \dots, N.$

Canonical moments [Dette and Studden, 1997]:

for fixed $\mathbf{c}_{k-1} = (c_1, \dots, c_{k-1})^t \in \overset{\circ}{\mathcal{M}}_{k-1}$, $c_k \in [c_k^-(\mathbf{c}_{k-1}), c_k^+(\mathbf{c}_{k-1})]$ and one denotes

$$p_k = \frac{c_k - c_k^-(\mathbf{c}_{k-1})}{c_k^+(\mathbf{c}_{k-1}) - c_k^-(\mathbf{c}_{k-1})} \in [0, 1],$$

$$p_1 = c_1, \quad p_2 = \frac{c_2 - c_1^2}{c_1(1 - c_1)}, \quad p_3 = \frac{(1 - c_1)(c_1 c_3 - c_2^2)}{(c_2 - c_1^2)(c_1 - c_2)}, \quad \dots$$

Moment space

 N^{th} moment space of probability measures on $[0, 1]$

$$\widetilde{\mathcal{M}}_N = \{\mathbf{c}_N(\mu) | \mu \in \mathcal{P}\}, \quad \mathbf{c}_N(\mu) = (c_1(\mu), \dots, c_N(\mu))^t, \quad c_k(\mu) = \int_0^1 x^k d\mu(x).$$

Hankel determinants:

$$\underline{H}_{2m+d} = \begin{vmatrix} c_d & \dots & c_{m+d} \\ \vdots & & \vdots \\ c_{m+d} & \dots & c_{2m+d} \end{vmatrix} \quad \overline{H}_{2m+d} = \begin{vmatrix} c_{1-d} - c_{2-d} & \dots & c_m - c_{m+1} \\ \vdots & \vdots & \vdots \\ c_m - c_{m+1} & \dots & c_{2m-1+d} - c_{2m+d} \end{vmatrix}$$

 $\mathcal{M} = (c_1, \dots, c_N) \in \widetilde{\mathcal{M}}_N \Leftrightarrow \underline{H}_i \geq 0 \text{ and } \overline{H}_i \geq 0 \text{ for } d = 0, 1 \text{ and } i = 0, \dots, N.$
 $\mathcal{M} = (c_1, \dots, c_N) \in \overset{\circ}{\widetilde{\mathcal{M}}}_N \Leftrightarrow \underline{H}_i > 0 \text{ and } \overline{H}_i > 0 \text{ for } d = 0, 1 \text{ and } i = 0, \dots, N.$

Canonical moments [Dette and Studden, 1997]:

$$p_1 = c_1, \quad p_2 = \frac{c_2 - c_1^2}{c_1(1 - c_1)}, \quad p_3 = \frac{(1 - c_1)(c_1 c_3 - c_2^2)}{(c_2 - c_1^2)(c_1 - c_2)}, \quad \dots$$

bijection between the interior of $\overset{\circ}{\widetilde{\mathcal{M}}}_N$ and $]0, 1[^N$

Reconstruction

Finite Hausdorff moment problem for the moment vector \mathcal{M}

find a non-negative real function $f_{\mathcal{M}}$ defined on $[0, 1]$ and such that

$$\mathcal{M} = \int_0^1 f_{\mathcal{M}}(x) \begin{pmatrix} 1 \\ x \\ \vdots \\ x^N \end{pmatrix} dx$$

Let us assume that \mathcal{M} belongs to the interior of $\mathcal{M}_N \rightarrow$ infinity of solutions

- **quadrature** solution as a sum of Dirac delta functions
- **polynomial** reconstruction [Laurent, 2006]
- reconstruction with a **sum of beta PDF** [Yuan et al., 2012]
- **Shannon's Entropy maximization** $H[f] = - \int_0^1 f(x) \ln f(x) dx$

[Mead and Papanicolaou, 1984, Tagliani, 1999, Massot et al., 2010]

$$\Rightarrow f(x) = \exp \left(- \sum_{j=0}^N \xi_j x^j \right)$$

The interior of the moment space is entirely attained (in theory).

Calcul of the ξ_j by an iterative Newton method

Calcul of the integrals by a Gauss-Legendre quadrature

Reconstruction

Finite Hausdorff moment problem for the moment vector \mathcal{M}

find a non-negative real function $f_{\mathcal{M}}$ defined on $[0, 1]$ and such that

$$\mathcal{M} = \int_0^1 f_{\mathcal{M}}(x) \begin{pmatrix} 1 \\ x \\ \vdots \\ x^N \end{pmatrix} dx$$

Let us assume that \mathcal{M} belongs to the interior of $\mathcal{M}_N \rightarrow$ infinity of solutions

- **quadrature** solution as a sum of Dirac delta functions
 - unique lower principle representation (minimization of M_{N+1})
 - not adapted for the computation of pointwise values or integrals on intervals strictly included in $]0, 1[$

- **polynomial** reconstruction [Laurent, 2006]

- reconstruction with a **sum of beta PDF** [Yuan et al., 2012]

- **Shannon's Entropy maximization** $H[f] = - \int_0^1 f(x) \ln f(x) dx$

[Mead and Papanicolaou, 1984, Tagliani, 1999, Massot et al., 2010]

$$\Rightarrow f(x) = \exp\left(-\sum_{j=0}^N \xi_j x^j\right)$$

Reconstruction

Finite Hausdorff moment problem for the moment vector \mathcal{M}

find a non-negative real function $f_{\mathcal{M}}$ defined on $[0, 1]$ and such that

$$\mathcal{M} = \int_0^1 f_{\mathcal{M}}(x) \begin{pmatrix} 1 \\ x \\ \vdots \\ x^N \end{pmatrix} dx$$

Let us assume that \mathcal{M} belongs to the interior of $\mathcal{M}_N \rightarrow$ infinity of solutions

- **quadrature** solution as a sum of Dirac delta functions
- **polynomial** reconstruction [Laurent, 2006]
 - $\rightarrow N + 1$ order of accuracy
 - \rightarrow Need more work for **positivity preserving** (done in the case $N = 1$ with a bi-affine reconstruction)
- reconstruction with a **sum of beta PDF** [Yuan et al., 2012]
- **Shannon's Entropy maximization** $H[f] = - \int_0^1 f(x) \ln f(x) dx$

[Mead and Papanicolaou, 1984, Tagliani, 1999, Massot et al., 2010]

$$\Rightarrow f(x) = \exp \left(- \sum_{j=0}^N \xi_j x^j \right)$$

Reconstruction

Finite Hausdorff moment problem for the moment vector \mathcal{M}

find a non-negative real function $f_{\mathcal{M}}$ defined on $[0, 1]$ and such that

$$\mathcal{M} = \int_0^1 f_{\mathcal{M}}(x) \begin{pmatrix} 1 \\ x \\ \vdots \\ x^N \end{pmatrix} dx$$

Let us assume that \mathcal{M} belongs to the interior of $\mathcal{M}_N \rightarrow$ infinity of solutions

- **quadrature** solution as a sum of Dirac delta functions
- **polynomial** reconstruction [Laurent, 2006]
- reconstruction with a **sum of beta PDF** [Yuan et al., 2012]

$$f(\xi) = \sum_{\alpha=1}^n w_{\alpha} \frac{\xi^{\frac{\xi_{\alpha}}{\sigma}-1} (1-\xi)^{\frac{1-\xi_{\alpha}}{\sigma}-1}}{B\left(\frac{\xi_{\alpha}}{\sigma}, \frac{1-\xi_{\alpha}}{\sigma}\right)}$$

\rightarrow one recover the quadrature when $\sigma \rightarrow 0$

\rightarrow eventually "lose" of the last moment

- **Shannon's Entropy maximization** $H[f] = - \int_0^1 f(x) \ln f(x) dx$

Reconstruction

Finite Hausdorff moment problem for the moment vector \mathcal{M}

find a non-negative real function $f_{\mathcal{M}}$ defined on $[0, 1]$ and such that

$$\mathcal{M} = \int_0^1 f_{\mathcal{M}}(x) \begin{pmatrix} 1 \\ x \\ \vdots \\ x^N \end{pmatrix} dx$$

Let us assume that \mathcal{M} belongs to the interior of $\mathcal{M}_N \rightarrow$ infinity of solutions

- **quadrature** solution as a sum of Dirac delta functions
- **polynomial** reconstruction [Laurent, 2006]
- reconstruction with a **sum of beta PDF** [Yuan et al., 2012]
- **Shannon's Entropy maximization** $H[f] = - \int_0^1 f(x) \ln f(x) dx$

[Mead and Papanicolaou, 1984, Tagliani, 1999, Massot et al., 2010]

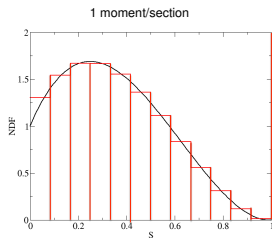
$$\Rightarrow f(x) = \exp \left(- \sum_{j=0}^N \xi_j x^j \right)$$

The interior of the moment space is entirely attained (in theory).

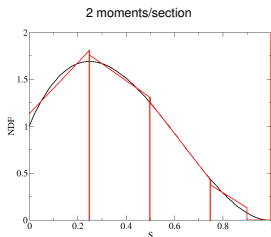
Calcul of the ξ_j by an iterative Newton method

Calcul of the integrals by a Gauss-Legendre quadrature

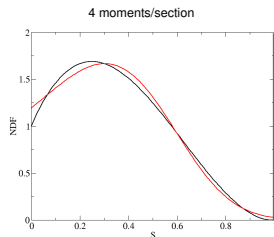
Examples of reconstructions



constant function in the
section
12 moments



bi-affine function
8 moments



entropy maximization
4 moments

increasing the number of size moments per section



decreasing the number of sections



decreasing the cost

increasing the model complexity



Robust algorithm for the resolution: purely evaporating case

System to solve:

$$d_t \mathcal{M} = -A \mathcal{M} - \phi_-, \quad \mathcal{M} = (\mathcal{M}_0, \dots, \mathcal{M}_N)^t$$

Integral version of the system

The integral form of the solution is written :

$$\exp(t A) \mathcal{M}(t) = \mathcal{M}(0) - \Psi_-(t), \quad \Psi_-(t) = \int_0^t f(0, \beta) \begin{bmatrix} 1 \\ \beta \\ \vdots \\ \beta^N \end{bmatrix} d\beta.$$

Algorithm

1. Reconstruction f_{ME} by entropy maximization and flux evaluation
2. Shift in size
3. Projection

Robust algorithm for the resolution: purely evaporating case

Integral version of the system

The integral form of the solution is written :

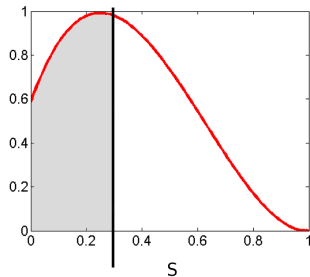
$$\exp(tA) \mathcal{M}(t) = \mathcal{M}(0) - \Psi_-(t), \quad \Psi_-(t) = \int_0^t f(0, \beta) \begin{bmatrix} 1 \\ \beta \\ \vdots \\ \beta^N \end{bmatrix} d\beta.$$

Algorithm

1. Reconstruction f_{ME} by entropy maximization and flux evaluation

$$\Psi_-(t) = \int_0^t f_{ME}(0, \beta) \begin{bmatrix} 1 \\ \beta \\ \vdots \\ \beta^N \end{bmatrix} d\beta.$$

2. Shift in size
3. Projection



Robust algorithm for the resolution: purely evaporating case

Integral version of the system

The integral form of the solution is written :

$$\exp(tA) \mathcal{M}(t) = \mathcal{M}(0) - \Psi_-(t), \quad \Psi_-(t) = \int_0^t f(0, \beta) \begin{bmatrix} 1 \\ \beta \\ \vdots \\ \beta^N \end{bmatrix} d\beta.$$

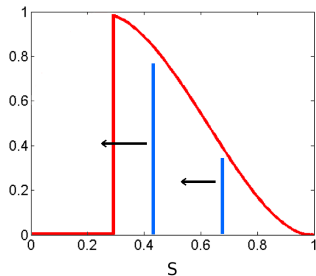
Algorithm

1. Reconstruction f_{ME} by entropy maximization and flux evaluation
2. Shift in size

$$\mathcal{M}_k(0) - \Psi_{k-}(t) = \sum_{i=1}^{(N+1)/2} w_i(0) S_i(0)^k, \quad \frac{dS_i}{dt} = -1$$

the abscissas $S_i(0)$ are in $[t, 1+t]$

3. Projection



Robust algorithm for the resolution: purely evaporating case

Integral version of the system

The integral form of the solution is written :

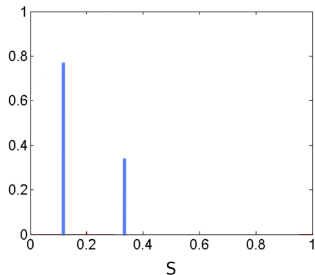
$$\exp(tA) \mathcal{M}(t) = \mathcal{M}(0) - \Psi_-(t), \quad \Psi_-(t) = \int_0^t f(0, \beta) \begin{bmatrix} 1 \\ \beta \\ \vdots \\ \beta^N \end{bmatrix} d\beta.$$

Algorithm

1. Reconstruction f_{ME} by entropy maximization and flux evaluation
2. Shift in size
3. Projection

$$\mathcal{M}_k(t) = \sum_{i=1}^{(N+1)/2} w_i(t) S_i(t)^k$$

$\mathcal{M}(t)$ is a moment vector!



Robust algorithm for the resolution: purely evaporating case

Integral version of the system

The integral form of the solution is written :

$$\exp(t A) \mathcal{M}(t) = \mathcal{M}(0) - \Psi_-(t), \quad \Psi_-(t) = \int_0^t f(0, \beta) \begin{bmatrix} 1 \\ \beta \\ \vdots \\ \beta^N \end{bmatrix} d\beta.$$

Algorithm

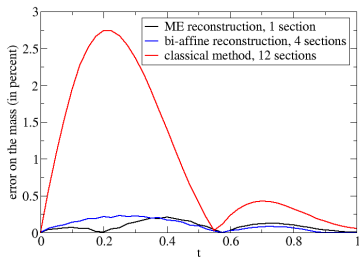
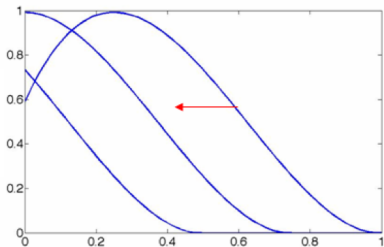
1. Reconstruction f_{ME} by entropy maximization and flux evaluation
2. Shift in size
3. Projection

generalized to any S dependent evaporation law

For $N=3$, the method is called EMSM (Eulerian Multi-Size Model)

[Massot et al., 2010]

Error on mass evolution



Error for the purely evaporating case

- EMSM more efficient than the classical method (1 moment/section) with 12 sections
- equivalent error between the second order method with 4 sections (8 moments) and the 4 moment method with 1 section
- EMSM highly decrease the computation cost compared to Multi-fluid model (in 2D, 36 moments for the Multi-fluid method, 6 moments for EMSM)

Advection scheme

General method: splitting between transport in physical space and transport in phase space.

→ the transport part has also to preserve the moment space

Kinetic model for purely advection case: $f(x, \mathbf{u}, S; t)$

$$\partial_t f + \mathbf{u} \cdot \partial_x f = 0$$

Monokinetic assumption: $f(\mathbf{x}, \mathbf{u}, S; t) = n(t, x, S)\delta(\mathbf{u} - \mathbf{u}_d(t, \mathbf{x}))$

$$\begin{cases} \partial_t(\mathcal{M}) + \partial_x(\mathcal{M}\mathbf{u}_d) = 0, \\ \partial_t(\mathcal{M}_1\mathbf{u}_d) + \partial_x(\mathcal{M}_1\mathbf{u}_d \otimes \mathbf{u}_d) = 0. \end{cases}$$

→ **weakly hyperbolic system** [Bouchut, 1994]

⇒ Kinetic finite volume scheme [Bouchut et al., 2003]

$$\begin{array}{ccc} \mathcal{M}_j^n, u_j^n & & \mathcal{M}_j^{n+1}, u_j^{n+1} \\ \downarrow & & \uparrow \\ f(x, u, S; t^n) & \xrightarrow[\Delta t]{\text{exact evolution}} & f(x, u, S; t^{n+1}) \end{array} \quad \text{with} \quad f(x, u, S; t^n) = f_{\mathcal{M}^n(x)}(S) \delta(u - u^n(x))$$

Difficulty: for the second order of accuracy, the x-reconstruction is not trivial

→ x-reconstruction of canonical moments [Kah et al 2012]

and use of a symbolic algebra software to determine the fluxes

Advection scheme

General method: splitting between transport in physical space and transport in phase space.

→ the transport part has also to preserve the moment space

Kinetic model for purely advection case: $f(\mathbf{x}, \mathbf{u}, S; t)$

$$\partial_t f + \mathbf{u} \cdot \partial_{\mathbf{x}} f = 0$$

Monokinetic assumption: $f(\mathbf{x}, \mathbf{u}, S; t) = n(t, \mathbf{x}, S) \delta(\mathbf{u} - \mathbf{u}_d(t, \mathbf{x}))$

$$\begin{cases} \partial_t(\mathcal{M}) + \partial_{\mathbf{x}}(\mathcal{M} \mathbf{u}_d) = 0, \\ \partial_t(\mathcal{M}_1 \mathbf{u}_d) + \partial_{\mathbf{x}}(\mathcal{M}_1 \mathbf{u}_d \otimes \mathbf{u}_d) = 0. \end{cases}$$

⇒ Kinetic finite volume scheme [Bouchut et al., 2003]

$$\begin{array}{ccc}
 \mathcal{M}_j^n, u_j^n & & \mathcal{M}_j^{n+1}, u_j^{n+1} \\
 \downarrow & & \uparrow \\
 f(\mathbf{x}, u, S; t^n) & \xrightarrow[\Delta t]{\text{exact evolution}} & f(\mathbf{x}, u, S; t^{n+1})
 \end{array}
 \quad \text{with} \quad
 f(\mathbf{x}, u, S; t^n) = f_{\mathcal{M}^n(\mathbf{x})}(S) \delta(u - u^n(\mathbf{x}))$$

Difficulty: for the second order of accuracy, the x-reconstruction is not trivial

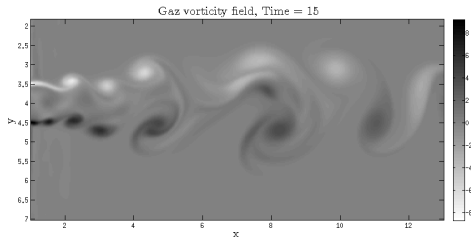
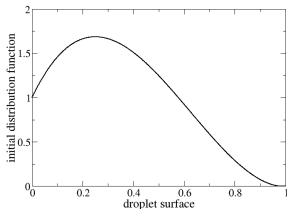
→ x-reconstruction of canonical moments [Kah et al 2012]

and use of a symbolic algebra software to determine the fluxes

Configuration

Free jets with polydisperse spray injection and evaporation [de Chaisemartin et al., 2009]

- Injection of a polydisperse spray in the center of the jet
- $Re=1000$ with a low level turbulence injection for destabilization purposes.
- Droplet distribution between Stokes = 0.03 and 0.75



Configuration

Free jets with polydisperse spray injection and evaporation [de Chaisemartin et al., 2009]

- Injection of a polydisperse spray in the center of the jet
- $Re=1000$ with a low level turbulence injection for destabilization purposes.
- Droplet distribution between Stokes = 0.03 and 0.75

Eulerian code MUSES3D [de Chaisemartin, 2009]

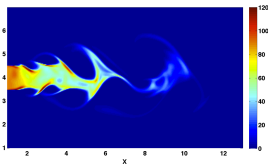
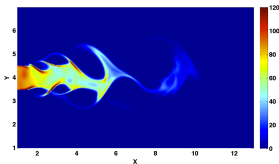
- Generic solver allowing implementation of new methods
- Fully parallelized (efficiency one on Certainty up to 512 cores)
- Coupling with a gaseous (Low Mach) + Lagrangian solver ASPHODELE from J. Reveillon, CORIA, Rouen
⇒ possibility of Eulerian and Lagrangian computation on the same gaseous field

Comparison with the Multi-fluid model

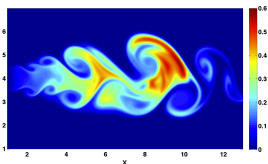
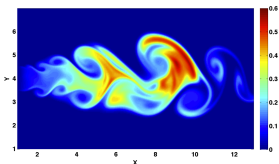
EMSM

Multi-Fluid with 10 sections

$m_{3/2}$



Y_F



Excellent agreement \Rightarrow validation of EMSM

EM reconstruction optimized up to the frontier of moment space
adaptive (Kah et al JCP 2012 - Vié et al JCP 2013)

Implementation in semi-industrial codes

CEDRE code (ONERA) (F. Doisneau, Collab. J. Dupays, A. Murrone)

- non-structured meshes (cell-center)
- DNS / LES
- Multi-fluid with two size moments

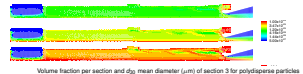
Two PhDs: F. Doisneau, A. Sibra Collab. J. Dupays

- first Multi-Fluid computations of a booster with coalescence
- improvement of the two-way coupling strategy - combustion of aluminium [Doisneau et al 2013, Doisneau et al 2014]

IFP-C3D code (IFPEn)

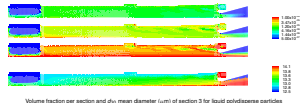
- moving meshes (ALE)
- RANS

polydisperse computation: selective repartition of droplets



30% overestimation of pressure
oscillation levels with
monodisperse computation

polydisperse computation with coalescence: significant influence of the coalescence



19% decreasing of pressure
oscillation levels with the
coalescence

Implementation in semi-industrial codes

CEDRE code (ONERA)

(F. Doisneau, Collab. J. Dupays, A. Murrone)

- non-structured meshes (cell-center)
- DNS / LES
- Multi-fluid with two size moments

IFP-C3D code (IFPEn)

- moving meshes (ALE)
- RANS
- EMSM with four size moments

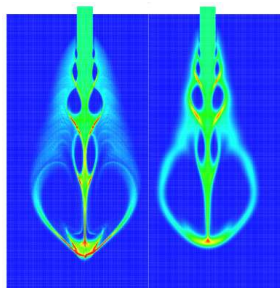
Two PhDs: D. Kah, O. Emre

Collab. S. Jay, S. de Chaisemartin, Q.-H Tran

- injection computations
- mesh movement with preservation of moment space [Kah et al 2014, Emre et al 2014, Emre et al 2015]

Lagrangian

EMSM



Implementation in semi-industrial codes

CEDRE code (ONERA)

(F. Doisneau, Collab. J. Dupays, A. Murrone)

- non-structured meshes (cell-center)
- DNS / LES
- Multi-fluid with two size moments

IFP-C3D code (IFPEn)

- moving meshes (ALE)
- RANS
- EMSM with four size moments

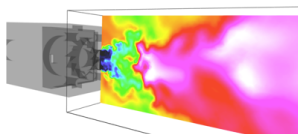
AVBP code (CERFACS and IFPEn)

- complex geometry
- non-structured meshes (cell vertex)
- LES (Vié et al 2013)

A. Vié

Collab. B. Cuenot

- first LES computations
(Multi-Fluid + MEF
formalism)



Outline

- 1 High order moment methods in size, with realizable and accurate numerical methods
- 2 High order moment methods in velocity, with realizable and accurate numerical methods
 - Up to second order moment methods (statistical crossing)
 - Higher order moment methods (deterministic crossing)
 - Multi-Gaussian model
- 3 Dealing with model coupling and asymptotic limits
 - A Hybrid model and related relaxation scheme
 - An Asymptotic-Preserving Relaxation scheme

Eulerian moment method

Mesoscopic description: simplified Williams-Boltzmann equation

Monodisperse, constant size and temperature [Williams 1958]

$$\partial_t f + \partial_x \cdot (\mathbf{u}f) + \partial_u \cdot (Ff) = 0, \quad F = \frac{\mathbf{U}_g - \mathbf{u}}{\tau_p} \quad (1)$$

Eulerian moment method

Mesoscopic description: simplified **Williams-Boltzmann equation**

Monodisperse, constant size and temperature [Williams 1958]

$$\partial_t f + \partial_{\mathbf{x}} \cdot (\mathbf{u}f) + \partial_{\mathbf{u}} \cdot (\mathbf{F}f) = 0, \quad \mathbf{F} = \frac{\mathbf{U}_g - \mathbf{u}}{\tau_p} \quad (1)$$

Macroscopic description: **moment equations**

Integrating (1) over the velocity phase space:

$$\partial_t \mathcal{M}_k + \partial_{\mathbf{x}} \cdot \mathcal{M}_{k+1} = k \frac{\mathcal{M}_{k-1} \odot \mathbf{U}_g - \mathcal{M}_k}{\tau_p} \quad (2)$$

where $\mathcal{M}_k = \int_{\mathbb{R}^d} (\otimes^k \mathbf{u}) f(t, \mathbf{x}, \mathbf{u}) d\mathbf{u}$

Closure problem: the highest order flux is unknown

Eulerian moment method

Mesoscopic description: simplified **Williams-Boltzmann equation**

Monodisperse, constant size and temperature [Williams 1958]

$$\partial_t f + \partial_{\mathbf{x}} \cdot (\mathbf{u}f) + \partial_{\mathbf{u}} \cdot (\mathbf{F}f) = 0, \quad \mathbf{F} = \frac{\mathbf{U}_g - \mathbf{u}}{\tau_p} \quad (1)$$

Macroscopic description: **moment equations**

Integrating (1) over the velocity phase space:

$$\partial_t \mathcal{M}_k + \partial_{\mathbf{x}} \cdot \mathcal{M}_{k+1} = k \frac{\mathcal{M}_{k-1} \odot \mathbf{U}_g - \mathcal{M}_k}{\tau_p} \quad (2)$$

$$\text{where } \mathcal{M}_k = \int_{\mathbb{R}^d} (\otimes^k \mathbf{u}) f(t, \mathbf{x}, \mathbf{u}) d\mathbf{u}$$

Closure problem: the highest order flux is unknown

Kinetic-Based Moment Method

Kinetic-Based Moment Method

$$\partial_t \mathcal{M}_k + \partial_{\mathbf{x}} \cdot \mathcal{M}_{k+1} = k \frac{\mathcal{M}_{k-1} \odot \mathbf{U}_g - \mathcal{M}_k}{\tau_p} \quad (3)$$

Closure: based on the choice of a presumed shape of the NDF (f)

- having as many parameters as the number of moments one needs to control

Advantages

- Coupling with the gas
- Parallel computing
- Well posed systems
- Direct link with the kinetic level

Challenges

- Numerical schemes
 - Realizability preservation

Realizability

Every set of moments has to be associated with a positive f

Kinetic-Based Moment Method

Kinetic-Based Moment Method

$$\partial_t \mathcal{M}_k + \partial_{\mathbf{x}} \cdot \mathcal{M}_{k+1} = k \frac{\mathcal{M}_{k-1} \odot \mathbf{U}_g - \mathcal{M}_k}{\tau_p} \quad (3)$$

Closure: based on the choice of a presumed shape of the NDF (f)

- having as many parameters as the number of moments one needs to control

Advantages

- Coupling with the gas
- Parallel computing
- Well posed systems
- Direct link with the kinetic level

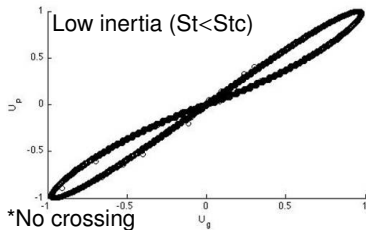
Challenges

- Numerical schemes
 - Realizability preservation

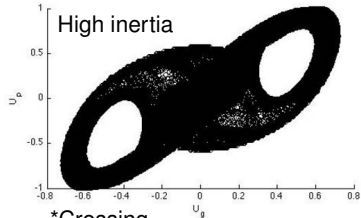
Realizability

Every set of moments has to be associated with a positive f

Kinetic-Based Moment Method



- *No crossing
- *High velocity correlation
- *Monokinetic



- *Crossing
- *Complex correlation
- *Polykinetic

Kinetic-Based Moment Method

M00	M10	M20	M30	M40
M01	M11	M21	M31	M41
M02	M12			
M03	M13			
M04	M14			

(Laurent et al. 2012)

StK=0

StK=1

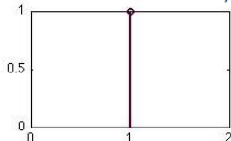
Stokes number \rightarrow

Zeroth order

■ Equilibrium Eulerian
 (Ferry et al. 2003)

First order

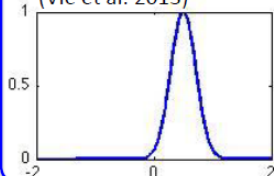
■ Monokinetic Assumption
 (Laurent & Massot 2001)



Second order

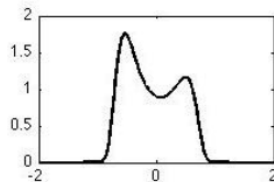
■ 2-Phi-EASM
 (Masi & Simonin 2012)

■ Anisotropic Gaussian
 (Vié et al. 2013)



Third and fourth order moments

■ CQMOM (Yuan & Fox 2010)
 ■ Multi-Gaussian
 (Chalons et al. 2010)



1 *Number of moments*

3 4

6 12

17

Outline

- 1 High order moment methods in size, with realizable and accurate numerical methods
- 2 High order moment methods in velocity, with realizable and accurate numerical methods
 - Up to second order moment methods (statistical crossing)
 - Higher order moment methods (deterministic crossing)
 - Multi-Gaussian model
- 3 Dealing with model coupling and asymptotic limits
 - A Hybrid model and related relaxation scheme
 - An Asymptotic-Preserving Relaxation scheme

Kinetic-Based Moment Method

Mono-Kinetic

$$f(t, \mathbf{x}, \mathbf{u}) = \rho(t, \mathbf{x})\delta(\mathbf{u} - \mathbf{u}_d(t, \mathbf{x}))$$

Anisotropic Gaussian

$$f(t, \mathbf{x}, \mathbf{u}) = \rho(t, \mathbf{x})\mathcal{N}(\mathbf{u} - \mathbf{u}_d, \Sigma)$$

Mono-Kinetic

$$\begin{cases} \partial_t \rho + \partial_{\mathbf{x}} \cdot (\rho \mathbf{u}_d) = 0 \\ \partial_t (\rho \mathbf{u}_d) + \partial_{\mathbf{x}} \cdot (\rho \mathbf{u}_d \otimes \mathbf{u}_d) = \frac{\rho(\mathbf{U}_g - \mathbf{u}_d)}{\tau_p} \end{cases}$$

- PGD (P=0) : weakly hyperbolic
- can generate δ -shocks and singularities: difficult to handle numerically
- reproduces the dynamics of low inertia particles with stiff accumulation and void regions

Kinetic-Based Moment Method

Mono-Kinetic

$$f(t, \mathbf{x}, \mathbf{u}) = \rho(t, \mathbf{x}) \delta(\mathbf{u} - \mathbf{u}_d(t, \mathbf{x}))$$

Anisotropic Gaussian

$$f(t, \mathbf{x}, \mathbf{u}) = \rho(t, \mathbf{x}) \mathcal{N}(\mathbf{u} - \mathbf{u}_d, \boldsymbol{\Sigma})$$

$$\mathcal{N} = \frac{\exp\left(-\frac{1}{2}(\mathbf{u} - \mathbf{u}_d)^T \boldsymbol{\Sigma}^{-1} (\mathbf{u} - \mathbf{u}_d)\right)}{(2\pi)^d |\boldsymbol{\Sigma}|^{1/2}}$$

Anisotropic-Gaussian

$$\begin{cases} \partial_t \rho + \partial_{\mathbf{x}} \cdot (\rho \mathbf{u}_d) = 0 \\ \partial_t (\rho \mathbf{u}_d) + \partial_{\mathbf{x}} \cdot (\rho \mathbf{u}_d \otimes \mathbf{u}_d + \mathbf{P}) = \frac{\rho(\mathbf{U}_g - \mathbf{u}_d)}{\tau_p} \\ \partial_t (\rho \mathbf{E}) + \partial_{\mathbf{x}} \cdot ((\rho \mathbf{E} + \mathbf{P}) \odot \mathbf{u}_d) = \frac{\rho(\mathbf{U}_g \odot \mathbf{u}_d - 2\mathbf{E})}{\tau_p} \end{cases}$$

where

- $\mathbf{E} = \frac{1}{2} \mathbf{u}_d \otimes \mathbf{u}_d + \frac{\mathbf{P}}{2\rho}$
- $\mathbf{P} = \rho \boldsymbol{\Sigma}$

- Entropy structure
- Hyperbolic

Kinetic-Based Moment Method

Mono-Kinetic

$$f(t, \mathbf{x}, \mathbf{u}) = \rho(t, \mathbf{x}) \delta(\mathbf{u} - \mathbf{u}_d(t, \mathbf{x}))$$

Anisotropic Gaussian

$$f(t, \mathbf{x}, \mathbf{u}) = \rho(t, \mathbf{x}) \mathcal{N}(\mathbf{u} - \mathbf{u}_d, \boldsymbol{\Sigma})$$

$$\mathcal{N} = \frac{\exp\left(-\frac{1}{2}(\mathbf{u} - \mathbf{u}_d)^T \boldsymbol{\Sigma}^{-1}(\mathbf{u} - \mathbf{u}_d)\right)}{(2\pi)^d |\boldsymbol{\Sigma}|^{1/2}}$$

Anisotropic-Gaussian

$$\begin{cases} \partial_t \rho + \partial_{\mathbf{x}} \cdot (\rho \mathbf{u}_d) = 0 \\ \partial_t (\rho \mathbf{u}_d) + \partial_{\mathbf{x}} \cdot (\rho \mathbf{u}_d \otimes \mathbf{u}_d + \mathbf{P}) = \frac{\rho(\mathbf{U}_g - \mathbf{u}_d)}{\tau_p} \\ \partial_t (\rho \mathbf{E}) + \partial_{\mathbf{x}} \cdot ((\rho \mathbf{E} + \mathbf{P}) \odot \mathbf{u}_d) = \frac{\rho(\mathbf{U}_g \odot \mathbf{u}_d - 2\mathbf{E})}{\tau_p} \end{cases}$$

where

- $\mathbf{E} = \frac{1}{2} \mathbf{u}_d \otimes \mathbf{u}_d + \frac{\mathbf{P}}{2\rho}$
- $\mathbf{P} = \rho \boldsymbol{\Sigma}$
- Entropy structure
- Hyperbolic

Kinetic-Based Moment Method

Isotropic Gaussian: Euler System

$$\begin{cases} \partial_t \rho + \partial_{\mathbf{x}} \cdot (\rho \mathbf{u}_d) = 0 \\ \partial_t (\rho \mathbf{u}_d) + \partial_{\mathbf{x}} \cdot (\rho \mathbf{u}_d \otimes \mathbf{u} + \mathbf{P}) = \frac{\rho(\mathbf{U}_g - \mathbf{u}_d)}{\tau_p} \\ \partial_t (\rho \mathcal{E}) + \partial_{\mathbf{x}} \cdot ((\rho \mathcal{E} + \mathcal{P}) \cdot \mathbf{u}_d) = \frac{\rho(\mathbf{U}_g \cdot \mathbf{u}_d - 2\mathcal{E})}{\tau_p} \end{cases}$$

with $\mathcal{E} = \text{tr}(\mathbf{E}) = \frac{1}{2} |\mathbf{u}_d|^2 + \sigma$, and $\mathbf{P} = \mathcal{P}\mathbf{I} = \rho\sigma\mathbf{I}$

$$\begin{cases} \partial_t \rho + \partial_{\mathbf{x}} \cdot (\rho \mathbf{u}_d) = 0 \\ \partial_t (\rho \mathbf{u}_d) + \partial_{\mathbf{x}} \cdot (\rho \mathbf{u}_d \otimes \mathbf{u}_d + \mathbf{P}) = \frac{\rho(\mathbf{U}_g - \mathbf{u}_d)}{\tau_p} \\ \partial_t (\rho \mathbf{E}) + \partial_{\mathbf{x}} \cdot ((\rho \mathbf{E} + \mathbf{P}) \odot \mathbf{u}_d) = \frac{\rho(\mathbf{U}_g \odot \mathbf{u}_d - 2\mathbf{E})}{\tau_p} \end{cases}$$

where

- $\mathbf{E} = \frac{1}{2} \mathbf{u}_d \otimes \mathbf{u}_d + \frac{\mathbf{P}}{2\rho}$
- $\mathbf{P} = \rho \Sigma$

- Entropy structure
- Hyperbolic

Numerical Scheme: FV MUSCL/HLL

Free transport in the x-direction:

$$\partial_t \mathbf{M} + \partial_x \mathcal{F}(\mathbf{M}) = 0$$

Structured Meshes

Directional Splitting

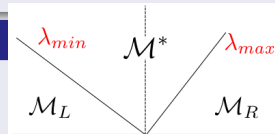
Realizability Preserving Numerical Flux \mathcal{F}^*

$$\mathbf{M}_{i-1}^n, \mathbf{M}_i^n, \mathbf{M}_{i+1}^n \in \mathcal{S} \Rightarrow \mathbf{M}_i^{n+1} \in \mathcal{S}$$

$$\mathbf{M}_i^{n+1} = \mathbf{M}_i^n - \frac{\Delta t}{|C_i|} \left(\mathcal{F}^*(\mathbf{M}_{i+1}^n, \mathbf{M}_i^n) - \mathcal{F}^*(\mathbf{M}_i^n, \mathbf{W}_{i-1}^n) \right)$$

Flux evaluation

$$\mathbf{M}^* = \frac{\mathbf{M}_L - \mathbf{M}_R}{\lambda_{min} - \lambda_{max}} - \frac{\mathcal{F}(\mathbf{M}_L) - \mathcal{F}(\mathbf{M}_R)}{\lambda_{min} - \lambda_{max}}$$



$$\mathcal{F}^{HLL} = \frac{1}{2} (\mathcal{F}(\mathbf{M}_L) + \mathcal{F}(\mathbf{M}_R)) - \frac{|\lambda_{min}|}{2} (\mathbf{M}^* - \mathbf{M}_L) - \frac{|\lambda_{max}|}{2} (\mathbf{M}_R - \mathbf{M}^*)$$

Numerical Scheme: FV MUSCL/HLL

Realizability (AG)

- $\rho > 0$,
- $p_{11} > 0, p_{22} > 0$,
- $p_{11}p_{22} - p_{12}^2 > 0$.

Realizable AND Conservative reconstruction

- Primitive Variables: $\mathbf{U} = (\rho, \mathbf{u}_d, \mathbf{P})$
- Realizable reconst.: $\mathbf{U}_j(x) = \overline{\mathbf{U}}_j + \mathbf{D}_U(x - x_j)$
- Conservative correction: $\int_{C_j} \mathbf{M}(\mathbf{U}_j(x)) = \overline{\mathbf{M}}_j$ imposed by the conservation of the cell value for each moment in order to ensure that the fluxes will not affect the realizability (Vié et al. 2015)

Time integration

SSP-RK2 Time Integration (Gottlieb et al. 2001)

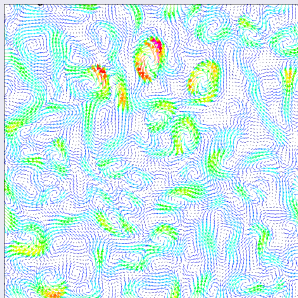
$$\mathbf{M}_i^{n+1} = \frac{\mathbf{M}_i^n}{2} + \frac{1}{2} \left[\mathbf{M}_i^{(1)} - \frac{\Delta t}{\Delta x} (\mathcal{F}_{i+1/2}^{(1)} - \mathcal{F}_{i-1/2}^{(1)}) \right]$$
$$\mathbf{M}_i^{(1)} = \mathbf{M}_i^n - \frac{1}{2} \frac{\Delta t}{\Delta x} (\mathcal{F}_{i+1/2}^n - \mathcal{F}_{i-1/2}^n)$$

- 2nd-order in space and time and realizable scheme, under CFL 0.5
 - $\mathbf{M}^n \in \mathcal{S} \Rightarrow \mathbf{M}^{n+1} \in \mathcal{S}$

2D DNS results

Test case

- Frozen HIT velocity field
- Homogeneous spray at $t=0$
- 2 Stokes numbers: 1 and 5



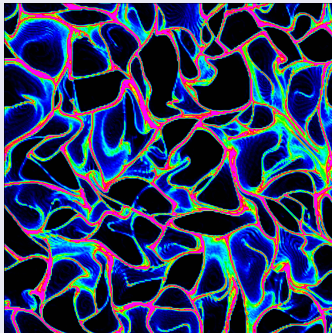
Results

- Snapshots of the number density
- Segregation vs. time for different models
- Segregation and MCE vs. St

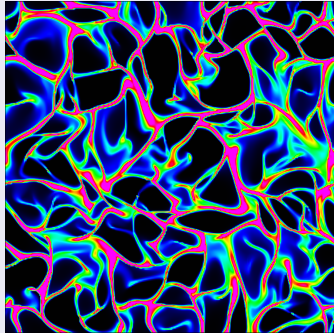
Segregation: spatial correlation of the number density field at a given cell size length

Number density Mesh 256^2 $St=1$

Lagrangian



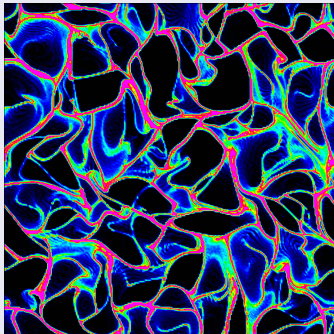
Mono-Kinetic



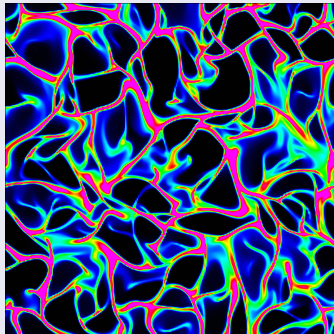
AG qualitatively match the Lagrangian results, no unphysical accumulations

Number density Mesh 256^2 $St=1$

Lagrangian



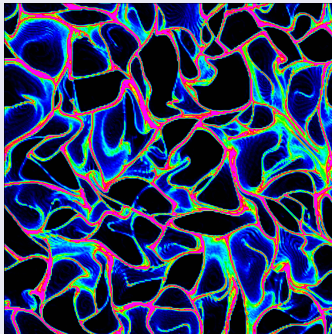
Isotropic Gaussian



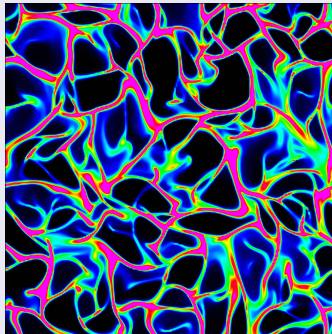
AG qualitatively match the Lagrangian results, no unphysical accumulations

Number density Mesh 256^2 $St=1$

Lagrangian



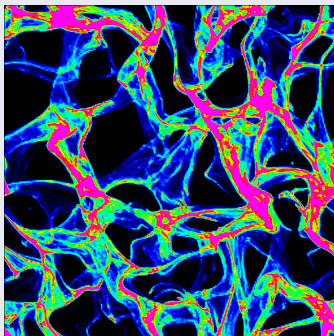
Anisotropic Gaussian



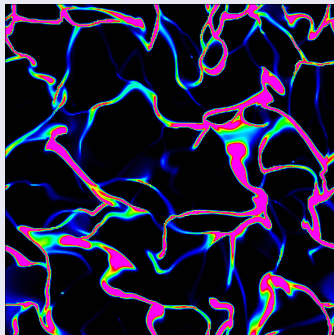
AG qualitatively match the Lagrangian results, no unphysical accumulations

Number density Mesh 256^2 $St=5$

Lagrangian



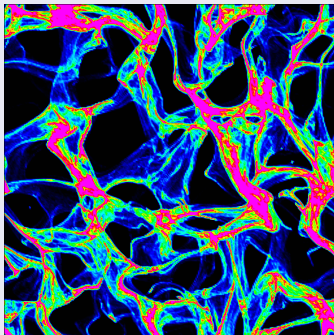
Mono-Kinetic



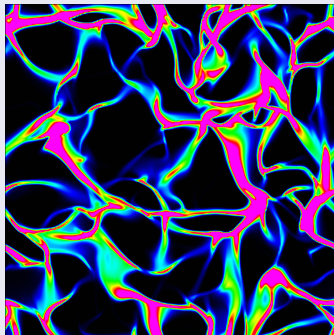
AG qualitatively match the Lagrangian results, no unphysical accumulations

Number density Mesh 256^2 $St=5$

Lagrangian



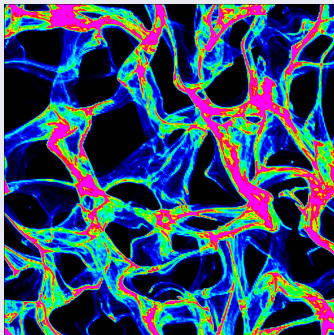
Isotropic Gaussian



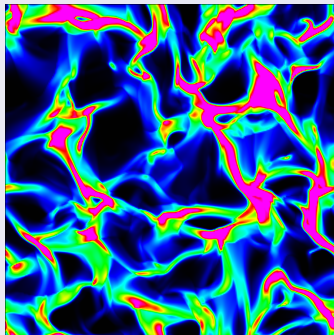
AG qualitatively match the Lagrangian results, no unphysical accumulations

Number density Mesh 256^2 $St=5$

Lagrangian

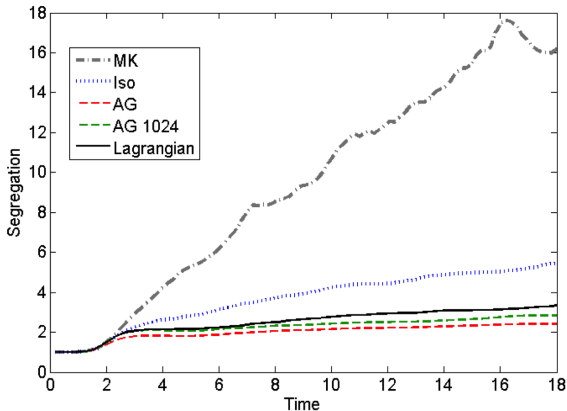


Anisotropic Gaussian



AG qualitatively match the Lagrangian results, no unphysical accumulations

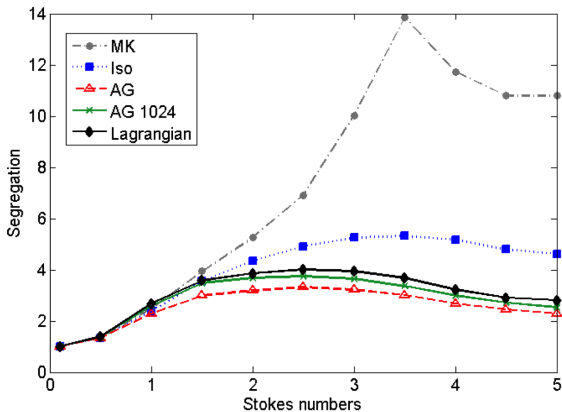
Segregation vs. time ($St=5$)



MK and Iso: greatly overestimate the segregation

AG: converge to Lagrangian

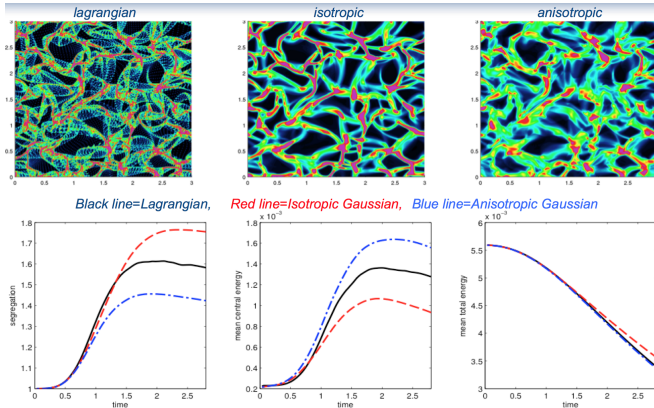
Segregation vs. St



AG: right behavior for the range of Stokes number studied

Taking into account statistical PTC

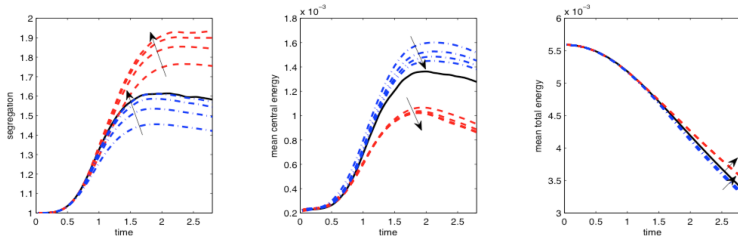
Lagrangian ref. solution - Isotropic Kinetic Closure - Gaussian Kinetic Closure



Stokes = 10 - Homogeneous Isotropic turbulence - density of particles
Vié, Doisneau, Massot, CICP 2015 - HLL realizable 2nd order in space and time.

Taking into account statistical PTC

Mesh refinement indicated the proper choice in terms of modeling



Black line=Lagrangian, Red line=Isotropic Gaussian, Blue line=Anisotropic Gaussian

Stokes = 10 - Homogeneous Isotropic turbulence - density of particles
Vié, Doisneau, Massot, CICP 2015 - HLL realizable 2nd order in space and time.

Taking into account statistical PTC

Lagrangian ref. solution - Gaussian Kinetic Closure - Algebraic Closure



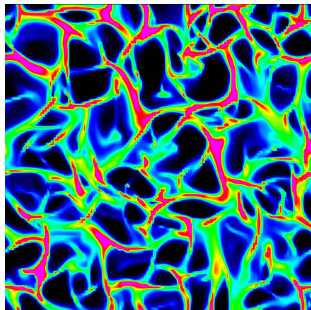
Stokes = 5 - Shear layer + Homogeneous Isotropic turbulence - density of particles

Vié, Masi, Simonin, Massot (Summer Program 2012 - Stanford University - CTR).

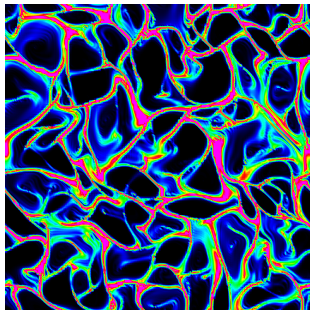
DNS (and LES) : Need to couple PGD and higher order moment methods

High order numerical schemes and unstructured meshes

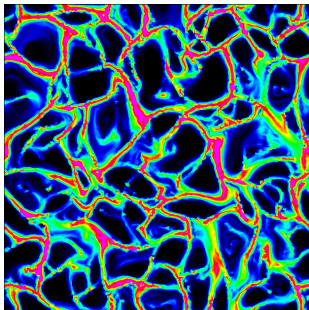
- 1D comparison of different numerical schemes (Larat et al. 2012, Sabat et al. 2015)
- Unstructured realizability preserving DG method (Larat et al. 2012, Sabat et al. 2014)



FV structured 128^2



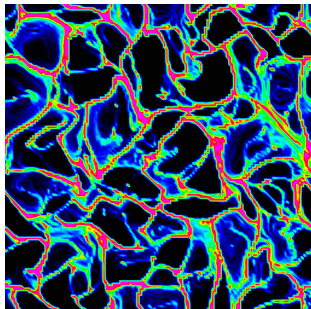
DG structured 128^2



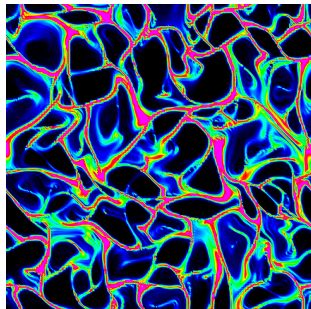
DG unstructured 64^2

High order numerical schemes and unstructured meshes

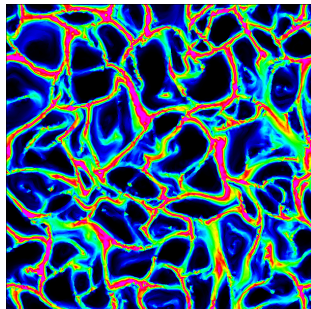
- 1D comparison of different numerical schemes (Larat et al. 2012, Sabat et al. 2015)
- Unstructured realizability preserving DG method (Larat et al. 2012, Sabat et al. 2014)



Lagrangian



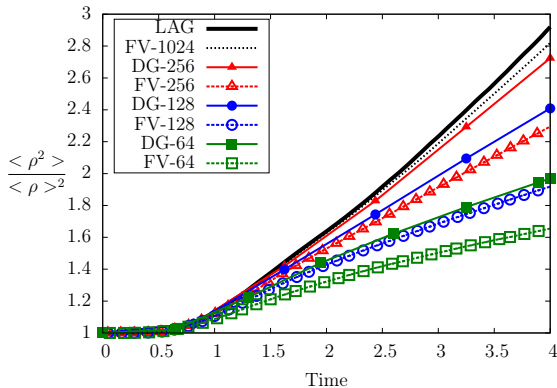
DG structured 128^2



DG unstructured 64^2

High order numerical schemes and unstructured meshes

- 1D comparison of different numerical schemes (Larat et al. 2012, Sabat et al. 2015)
- Unstructured realizability preserving DG method (Larat et al. 2012, Sabat et al. 2014)



Outline

- 1 High order moment methods in size, with realizable and accurate numerical methods
- 2 High order moment methods in velocity, with realizable and accurate numerical methods
 - Up to second order moment methods (statistical crossing)
 - Higher order moment methods (deterministic crossing)
 - Multi-Gaussian model
- 3 Dealing with model coupling and asymptotic limits
 - A Hybrid model and related relaxation scheme
 - An Asymptotic-Preserving Relaxation scheme

Moment method in velocity

Simplified and dimensionless kinetic model

$f(\mathbf{x}, \mathbf{u}; t)$: number density function (NDF)

Williams - Boltzmann transport equation

$$\partial_t f + \partial_{\mathbf{x}} \cdot (\mathbf{u} f) + \partial_{\mathbf{u}} \cdot \left(\frac{\mathbf{U}_g - \mathbf{u}}{\text{St}} f \right) = 0$$

Eulerian description

- Moments of the NDF:

$$M^j = \int \mathbf{u}^j f(\mathbf{x}, \mathbf{u}; t) d\mathbf{u} = \int u_1^{j_1} \dots u_d^{j_d} f(\mathbf{x}, \mathbf{u}; t) du_1 \dots du_d$$

- moment vector: $\mathcal{M} = (M^j)_{j \in \mathcal{S}}$, \mathcal{S} finite subset of \mathbb{N}^d
- equations on \mathcal{M}

example in 1D:

$$\partial_t M^j + \partial_x M^{j+1} = \frac{U_g M^{j-1} - M^j}{\text{St}}$$

→ need a closure for M^{N+1}

Closure

Objective

Express higher order moments as a function of the moment vector \mathcal{M}

1D case

Finite Hamburger moment problem for the moment vector \mathcal{M} :

for $\mathcal{M} = (M^0, M^1, \dots, M^N)^t$, find a non-negative real function $f_{\mathcal{M}}$ defined on \mathbb{R} such that

$$\forall j \in \{0, 1, \dots, N\} \quad M^j = \int u^j f_{\mathcal{M}}(x, u; t) du$$

Hankel determinants:

$$H_m = \begin{vmatrix} M^0 & \dots & M^{m-1} \\ \vdots & & \vdots \\ M^{m-1} & \dots & M^{2m-2} \end{vmatrix}$$

the problem has a solution (an infinity in fact) if $H_m > 0$ for $m = 1, \dots, N + 1$.

2D/3D case

Problem:

for $\mathcal{M} = (M^i)$ find a non-negative real function f defined on \mathbb{R}^d such that

Closure

Objective

Express higher order moments as a function of the moment vector \mathcal{M}

1D case

Finite Hamburger moment problem for the moment vector \mathcal{M} :

for $\mathcal{M} = (M^0, M^1, \dots, M^N)^t$, find a non-negative real function $f_{\mathcal{M}}$ defined on \mathbb{R} such that

$$\forall j \in \{0, 1, \dots, N\} \quad M^j = \int u^j f_{\mathcal{M}}(x, u; t) du$$

2D/3D case

Problem:

for $\mathcal{M} = (M^j)_{j \in S}$, find a non-negative real function $f_{\mathcal{M}}$ defined on \mathbb{R} such that

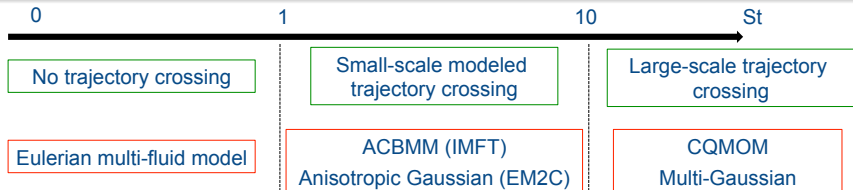
$$\forall j \in S \quad M^j = \int u^j f_{\mathcal{M}}(\mathbf{x}, \mathbf{u}; t) d\mathbf{u}$$

Theoretical difficulties:

→ choice S

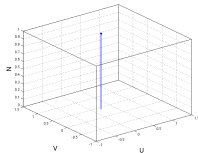
→ existence of solutions

Closure examples



Monokinetic assumption

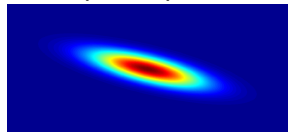
[de Chaisemartin, 2009]



Algebraic-Closure-Based

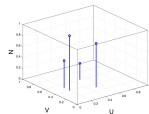
[Simonin et al., 2002, Masi and Simonin, 2012]

Anisotropic Gaussian closure [Vié et al 2015]



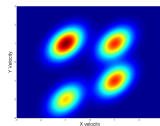
Quadrature closure

[Fox et al., 2008, de Chaisemartin et al., 2009,
Yuan et al 2011, Chalons et al., 2012]



Multi-Gaussian closure

[Chalons et al., 2013]



Outline

- 1 High order moment methods in size, with realizable and accurate numerical methods
- 2 High order moment methods in velocity, with realizable and accurate numerical methods
 - Up to second order moment methods (statistical crossing)
 - Higher order moment methods (deterministic crossing)
 - **Multi-Gaussian model**
- 3 Dealing with model coupling and asymptotic limits
 - A Hybrid model and related relaxation scheme
 - An Asymptotic-Preserving Relaxation scheme

Multi-gaussian closure - 1D case

model for advection: $\partial_t f + \partial_x(uf) = 0$

$$\partial_t \mathcal{M} + \partial_x \mathcal{F}(\mathcal{M}) = 0$$

Moment vector: $\mathcal{M} = (M^0, M^1, M^2, M^3, M^4)^t$ Flux $\mathcal{F}(\mathcal{M}) = (M^1, M^2, M^3, M^4, \bar{M}^5)^t$ Centered norm. moments on M^1 / M^0

$$e = \frac{M^0 M^2 - (M^1)^2}{(M^0)^2}$$

$$q = \frac{(M^3(M^0)^2 - (M^1)^3) - 3M^1(M^0 M^2 - (M^1)^2)}{(M^0)^3}$$

$$\eta = \frac{-3(M^1)^4 + M^4(M^0)^3 - 4(M^0)^2 M^1 M^3 + 6M^0(M^1)^2 M^2}{(M^0)^4}$$

Closure

$$f^G(u) = \sum_{\alpha=1}^2 \frac{\rho_\alpha}{\sigma \sqrt{2\pi}} \exp\left(-\frac{(u - u_\alpha)^2}{2\sigma^2}\right)$$

with ρ_1, ρ_2, u_1, u_2 and σ such that

$$\forall j \in \{0, 1, 2, 3, 4\} \quad \int_{\mathbb{R}} u^j f^G(u) du = M^j$$

and

$$\bar{M}^5 = \int_{\mathbb{R}} u^5 f^G(u) du$$

Proposition

Be $\Omega = \left\{ \mathcal{M}, M^0 > 0, e > 0, \eta > e^2 + \frac{q^2}{e}, \text{ and } \eta \leq 3e^2 \text{ if } q = 0 \right\}$.

Setting $\mathbf{U} = (\rho_1, \rho_2, \rho_1 u_1, \rho_2 u_2, \sigma)^t$, the function $\mathbf{U} = \mathbf{U}(\mathcal{M})$ is one-to-one and onto when $u_1 \neq u_2$, provided that we set $\rho_1 = \rho_2$ in the case $u_1 = u_2$. Moreover, σ^2 the unique real root of the polynomial $\mathcal{P} = 2(X - e)^3 + (\eta - 3e^2)(X - e) + q^2$.

Multi-gaussian closure - 1D case

model for advection: $\partial_t f + \partial_x(uf) = 0$

$$\partial_t \mathcal{M} + \partial_x \mathcal{F}(\mathcal{M}) = 0$$

Moment vector: $\mathcal{M} = (M^0, M^1, M^2, M^3, M^4)^t$

Flux $\mathcal{F}(\mathcal{M}) = (M^1, M^2, M^3, M^4, \bar{M}^5)^t$

Centered norm. moments on M^1/M^0

$$e = \frac{M^0 M^2 - (M^1)^2}{(M^0)^2},$$

$$q = \frac{(M^3(M^0)^2 - (M^1)^3) - 3M^1(M^0 M^2 - (M^1)^2)}{(M^0)^3}$$

$$\eta = \frac{-3(M^1)^4 + M^4(M^0)^3 - 4(M^0)^2 M^1 M^3 + 6M^0(M^1)^2 M^2}{(M^0)^4}.$$

Closure

$$f^G(u) = \sum_{\alpha=1}^2 \frac{\rho_\alpha}{\sigma \sqrt{2\pi}} \exp\left(-\frac{(u-u_\alpha)^2}{2\sigma^2}\right)$$

with ρ_1, ρ_2, u_1, u_2 and σ such that

$$\forall j \in \{0, 1, 2, 3, 4\} \quad \int_{\mathbb{R}} u^j f^G(u) du = M^j$$

and

$$\bar{M}^5 = \int_{\mathbb{R}} u^5 f^G(u) du$$

Proposition

Be $\Omega = \left\{ \mathcal{M}, M^0 > 0, e > 0, \eta > e^2 + \frac{q^2}{e}, \text{ and } \eta \leq 3e^2 \text{ if } q = 0 \right\}$.

Setting $\mathbf{U} = (\rho_1, \rho_2, \rho_1 u_1, \rho_2 u_2, \sigma)^t$, the function $\mathbf{U} = \mathbf{U}(\mathcal{M})$ is one-to-one and onto when $u_1 \neq u_2$, provided that we set $\rho_1 = \rho_2$ in the case $u_1 = u_2$. Moreover, σ^2 the unique real root of the polynomial $\mathcal{P} = 2(X - e)^3 + (\eta - 3e^2)(X - e) + q^2$.

Computation algorithm

Step 1: computation of σ

Finding the unique real root of

$$\mathcal{P} = 2(X - e)^3 + (\eta - 3e^2)(X - e) + q^2$$

→ A limiter is added to control the maximal value of the eigenvalues

Step 2: computation of ρ_1, ρ_2, u_1, u_2

One solves:

$$M^0 = \rho_1 + \rho_2,$$

$$M^1 = \rho_1 u_1 + \rho_2 u_2,$$

$$M^2 - \sigma^2 M^0 = \rho_1 u_1^2 + \rho_2 u_2^2,$$

$$M^3 - 3\sigma^2 M^1 = \rho_1 u_1^3 + \rho_2 u_2^3,$$

→ Quadrature algorithm for computation of abscissas and weights (or analytical formula).

System property

Model

$$\partial_t \mathcal{M} + \partial_x \mathcal{F}(\mathcal{M}) = 0 \quad (4)$$

Moment vector: $\mathcal{M} = (M^0, M^1, M^2, M^3, M^4)^t$

Flux $\mathcal{F}(\mathcal{M}) = (M^1, M^2, M^3, M^4, \bar{M}^5)^t$

Closure

$$f_M^G(u) = \sum_{\alpha=1}^2 \frac{\rho_\alpha}{\sigma \sqrt{2\pi}} \exp\left(-\frac{(u - u_\alpha)^2}{2\sigma^2}\right)$$

with ρ_1, ρ_2, u_1, u_2 and σ tels que

$$\forall j \in \{0, 1, 2, 3, 4\} \quad \int_{\mathbb{R}} u^j f^G(u) du = M^j$$

and

$$\bar{M}^5 = \int_{\mathbb{R}} u^5 f^G(u) du$$

Théorème

Assuming that $\mathcal{M} = (M_0, M_1, M_2, M_3, M_4)^t$ lives in Ω , then the system (4) is *hyperbolic*.

Numerical scheme

Kinetic Flux-Splitting scheme

- Finite volumes:

$$\mathcal{M}_c^n = \frac{1}{\Delta x} \int_{x_{c-1/2}}^{x_{c+1/2}} \mathcal{M}(t^n, x) dx$$

- Conservative

$$\mathcal{M}_c^{n+1} = \mathcal{M}_c^n - \frac{\Delta t}{\Delta x} (\mathcal{F}_{c+1/2} - \mathcal{F}_{c-1/2})$$

- Upwind scheme at the kinetic level
- Flux splitting:

$$\mathcal{F}_{c+1/2} = \mathcal{F}_{c+1/2}^+ + \mathcal{F}_{c+1/2}^-$$

$$(\mathcal{F}_{c+1/2}^+)^i = \int_0^{\infty} f_{\mathcal{M}_c^n}^G(u) u^{i+1} du,$$

$$(\mathcal{F}_{c+1/2}^-)^i = \int_{-\infty}^0 f_{\mathcal{M}_{c+1}^n}^G(u) u^{i+1} du.$$

→ Realizability

Results - Riemann problem

1D Riemann problem

Two homogeneous sprays, initially at equilibrium, which are crossing.

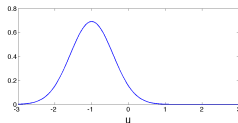
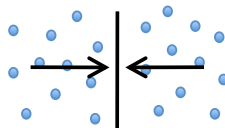
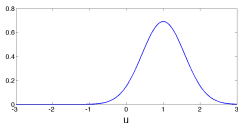
Initial conditions

$$M^0 = 1 \quad e = \frac{1}{3} \quad q = 0 \quad \eta = \frac{1}{3}$$

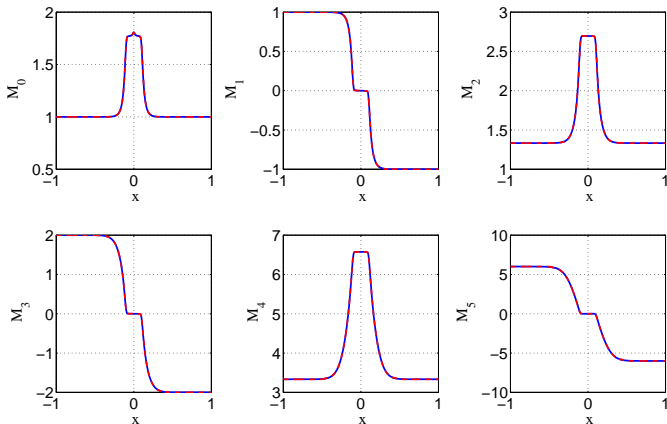
and

$$U_m = \frac{M_1}{M_0} = \begin{cases} 1 & \text{if } x < 0, \\ -1 & \text{otherwise.} \end{cases}$$

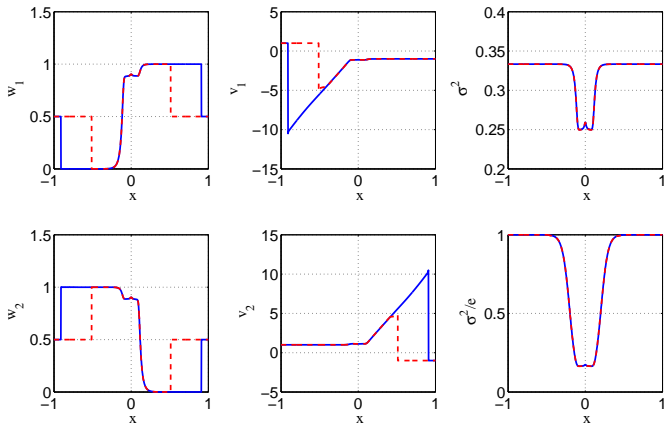
$t = 0$:



Results - Riemann problem

 $t = 0.5$: computed and reconstructed moments

Results - Riemann problem

 $t = 0.5$: abscissas, weights, σ^2 

Limiters on σ^2 : abscissas are bounded with a neglectable effect on moments

Multi-gaussian model - 2D case

Ingredients:

- dimensionnal splitting

- conditionnal quadrature [Yuan et al 2011] $M^{i,j} = \int v^j f(v|u) \int u^i f(u) du dv$

Equations in the x direction

$$\partial_t M^{i,j} + \partial_x M^{i+1,j} = 0$$

Set of moments

$$\begin{bmatrix} \mathbf{M}^{0,0} & \mathbf{M}^{0,1} & \mathbf{M}^{0,2} & \mathbf{M}^{0,3} & \mathbf{M}^{0,4} \\ \mathbf{M}^{1,0} & \mathbf{M}^{1,1} & \mathbf{M}^{1,2} & \mathbf{M}^{1,3} & \mathbf{M}^{1,4} \\ \mathbf{M}^{2,0} & \mathbf{M}^{2,1} & & & \\ \mathbf{M}^{3,0} & \mathbf{M}^{3,1} & & & \\ \mathbf{M}^{4,0} & \mathbf{M}^{4,1} & & & \end{bmatrix}.$$



Hyperbolic
system

Kinetic description

$$f_{12}(t, x, u, v) = \sum_{\alpha=1}^2 \sum_{\beta=1}^2 \rho_{\alpha} \rho_{\alpha\beta} g(u; u_{\alpha}, \sigma_{1}) g(v; v_{\alpha\beta}, \sigma_{2\alpha}),$$

with the Gaussian function: $g(u; \mu, \sigma) = \frac{1}{\sigma \sqrt{2\pi}} \exp\left(-\frac{(u - \mu)^2}{2\sigma^2}\right)$.

→ computation of three 1D multi-gaussian closures

Multi-gaussian model - 2D case

Ingredients:

- dimensionnal splitting

- conditionnal quadrature [Yuan et al 2011] $M^{i,j} = \int v^j f(v|u) \int u^i f(u) du dv$

Equations in the x direction

$$\partial_t M^{i,j} + \partial_x M^{i+1,j} = 0$$

Set of moments

$$\begin{bmatrix} \mathbf{M}^{0,0} & \mathbf{M}^{0,1} & \mathbf{M}^{0,2} & \mathbf{M}^{0,3} & \mathbf{M}^{0,4} \\ \mathbf{M}^{1,0} & \mathbf{M}^{1,1} & \mathbf{M}^{1,2} & \mathbf{M}^{1,3} & \mathbf{M}^{1,4} \\ \mathbf{M}^{2,0} & \mathbf{M}^{2,1} & & & \\ \mathbf{M}^{3,0} & \mathbf{M}^{3,1} & & & \\ \mathbf{M}^{4,0} & \mathbf{M}^{4,1} & & & \end{bmatrix}.$$

→

Hyperbolic
system

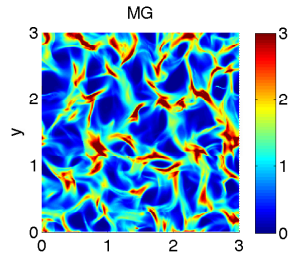
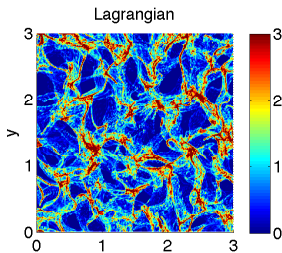
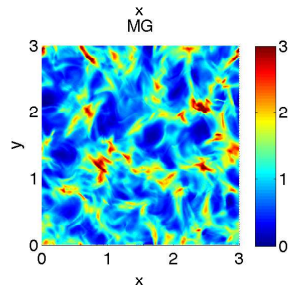
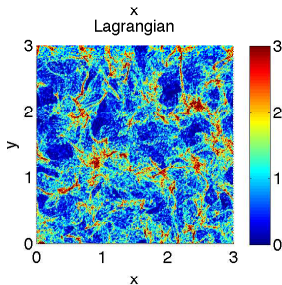
Kinetic description

$$f_{12}(t, x, u, v) = \sum_{\alpha=1}^2 \sum_{\beta=1}^2 \rho_{\alpha} \rho_{\alpha\beta} g(u; u_{\alpha}, \sigma_{1}) g(v; v_{\alpha\beta}, \sigma_{2\alpha}),$$

with the Gaussian function: $g(u; \mu, \sigma) = \frac{1}{\sigma \sqrt{2\pi}} \exp\left(-\frac{(u - \mu)^2}{2\sigma^2}\right).$

→ computation of three 1D multi-gaussian closures

Results - numerical comparisons on a 2D HIT

 $St = 5$  $St = 10$ 

Good agreement

Outline

- 1 High order moment methods in size, with realizable and accurate numerical methods
- 2 High order moment methods in velocity, with realizable and accurate numerical methods
 - Up to second order moment methods (statistical crossing)
 - Higher order moment methods (deterministic crossing)
 - Multi-Gaussian model
- 3 **Dealing with model coupling and asymptotic limits**
 - A Hybrid model and related relaxation scheme
 - An Asymptotic-Preserving Relaxation scheme

Main goal

Eulerian Large Eddy Simulation of turbulent polydisperse two-phase flows

Turbulence DNS and LES

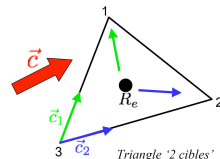
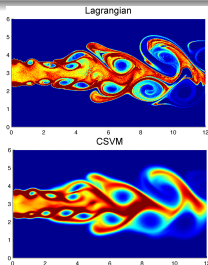
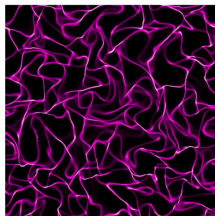
- Trajectory crossings
- Subgrid scale motion

Polydispersion

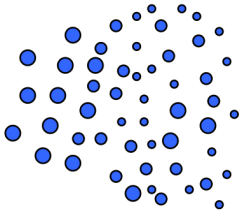
- Evaporation
- Coalescence, break-up
- Drag force
- Transport

Numerical methods

- Realizable
- Robust
- Arbitrary elements
- High order



Two-phase flow modeling



Williams-Boltzmann equation for the Number Density Function (NDF)

$$\frac{\partial f}{\partial t} + v_m \frac{\partial f}{\partial x_m} + \frac{\partial}{\partial v_m} \left(\frac{u_{g,m} - v_m}{St} f \right) = 0$$

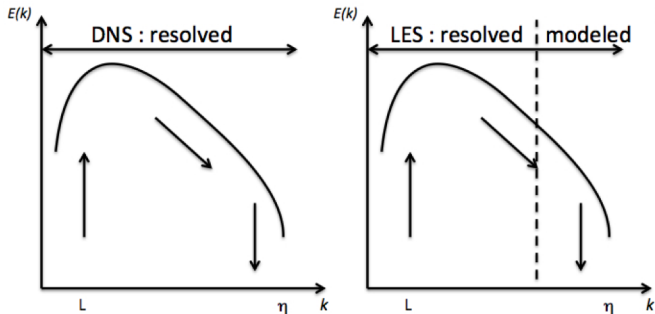
Eulerian description

- Moments of the NDF $M_{ijk} = \int u^i v^j w^k f(t, \mathbf{x}, \mathbf{v}) d\mathbf{v}$
- System of conservation equations on moments

Large Eddy Simulation

Why Large Eddy Simulation?

Because in industrial applications, Direct Numerical Simulations are unreachable, due to the large spectrum of size and time scales in the flow.



Large Eddy Simulation of disperse phase flows

The classical way: filtering at the moment level (Moreau et al. 2010)

- Integration of the WBE in velocity to obtain the moment equations (ME)
- Filtering of the moment equations

$$\text{WBE} \quad \frac{\partial f}{\partial t} + v_m \frac{\partial f}{\partial x_m} + \frac{\partial}{\partial v_m} \left(\frac{u_{g,m} - v_m}{St} f \right) = 0$$

$$\text{ME} \quad \frac{\partial M^i}{\partial t} + \frac{\partial}{\partial x} (M^{i+1}) = -\frac{i}{St} (M^i - u_g M^{i-1})$$

$$\text{filtered ME} \quad \frac{\partial \bar{M}^i}{\partial t} + \frac{\partial}{\partial x} (\bar{M}^{i+1}) = -\frac{i}{St} (\bar{M}^i - \overline{u_g M^{i-1}})$$

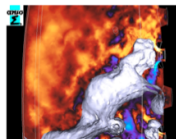
Problem

Designing realizable numerical methods is difficult, as the structure of the resulting system of equations is difficult to determine.

Large Eddy Simulation of disperse phase flows

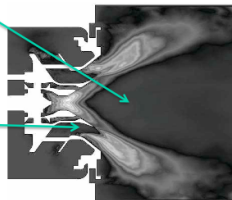
Février, Simonin et al. 2002, 2005

- 1st and trace of the 2nd order velocity moments of the NDF => moderate Stokes numbers, can handle first uncorrelated motion at the DNS level and then LES subgrid scale after filtering
- **Monodisperse**: $f(t, \mathbf{x}, \mathbf{u}, \delta) \rightarrow f(t, \mathbf{x}, \mathbf{u})$
(see Vié et al. ICMF 2010, FTC 2012 for extension to polydisperse)
- Extended to **LES of spray combustion**
- Implemented in the LES solver **AVBP: massively parallel** computing of industrial applications (See Boileau et al. 2008)



Spray ignition - Cerfacs

Kinetic energy in a multi-point gas turbine injector Jeagle 09



- For low Stokes numbers, or very weak turbulent energy, the model does not degenerate to **PGD**
- Resulting **shocks and δ -shocks** are very delicate to handle with the standard centered schemes used for LES
- **Vacuum** regions cannot be treated exactly

Large Eddy Simulation of disperse phase flows

An other way: filtering at the kinetic level (Reeks 1991, Zaichik et al. 2009)

- Filtering of the kinetic equation
- Integration of the filtering WBE in velocity to obtain the moment equations

$$\text{WBE} \quad \frac{\partial f}{\partial t} + v_m \frac{\partial f}{\partial x_m} + \frac{\partial}{\partial v_m} \left(\frac{u_{g,m} - v_m}{St} f \right) = 0$$

$$\text{filtered WBE} \quad \frac{\partial \bar{f}}{\partial t} + c_p \frac{\partial \bar{f}}{\partial x} + \frac{\partial}{\partial c_p} \left[\frac{\bar{u}_g - c_p}{St} f \right] = \frac{\partial}{\partial c_p} \left[\lambda \frac{\partial \bar{f}}{\partial x} + \mu \frac{\partial \bar{f}}{\partial c_p} \right]$$

$$\text{filtered ME} \quad \frac{\partial \bar{M}^i}{\partial t} + \frac{\partial}{\partial x} \left(\bar{M}^{i+1} + i\lambda \bar{M}^{i-1} \right) = -\frac{i}{St} \left(\bar{M}^i - \bar{u}_g \bar{M}^{i-1} - (i-1) St \mu \bar{M}^{i-2} \right)$$

Good news

This method leads to an hyperbolic system of equations with source terms, with a well-defined underlying kinetic equation, really helpful to design realizable methods. PhD Macole Sabat 2015, Sabat et al 2015

Gaussian closure and 3-equation system

$$\frac{\partial \bar{M}^i}{\partial t} + \frac{\partial}{\partial x} \left(\bar{M}^{i+1} + i\lambda \bar{M}^{i-1} \right) = -\frac{i}{St} \left(\bar{M}^i - \bar{u}_g \bar{M}^{i-1} - (i-1) St \mu \bar{M}^{i-2} \right)$$

Closure problem

For a given set of moments $M^{0,\dots,N}$, the moment M^{N+1} is needed.

Here we propose to use a Gaussian closure:

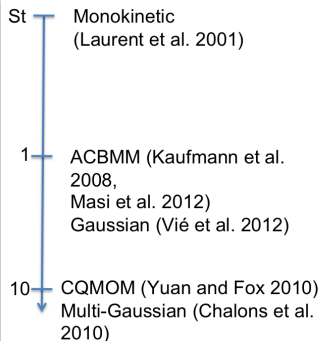
$$f(t, x, c_p) = \frac{\rho(t, x)}{\sqrt{4\pi\varepsilon(t, x)}} \exp\left(-\frac{(c_p - u(t, x))^2}{4\varepsilon(t, x)}\right)$$

for which 3 parameters are needed: ρ , u and ε .

Interest of the Gaussian closure for two-phase flows

Capture primary aspects trajectory crossings that occurs in turbulent flows

Enable to simulate turbulent flows at Stokes numbers close to 1



Gaussian closure and 3-equation system

Euler-like system of equations

$$\begin{aligned}\frac{\partial \rho}{\partial t} + \frac{\partial \rho u}{\partial x} &= 0 \\ \frac{\partial \rho u}{\partial t} + \frac{\partial \rho u^2 + P}{\partial x} &= -\frac{\rho(u - \bar{u}_g)}{St} \\ \frac{\partial \rho E}{\partial t} + \frac{\partial \rho u E + P}{\partial x} &= -\frac{\rho u(u - \bar{u}_g)}{St} - \frac{\rho(2\varepsilon - St\mu)}{St}\end{aligned}$$

where:

$$\rho = M^0, \quad \rho u = M^1, \quad \rho E = \frac{1}{2}M^2, \quad \rho\varepsilon = M^2 - M^0 u^2, \quad P = 2\rho\varepsilon + \rho\lambda$$

The subgrid scale influence is seen on the source terms as well as on the pressure law

Asymptotic behavior

Considering the expression of λ and μ :

$$\lambda = \frac{\tau_g}{St(1 + St)}, \quad \mu = \frac{\tau_g}{St(1 + St)}$$

where τ_g is the subgrid scale energy of the gas phase.

Sound speed

The sound speed tends to infinity when St tends to 0:

$$c = \sqrt{6\varepsilon + 3\lambda} \xrightarrow[St \rightarrow 0]{} \infty$$

One may want to treat the acoustic part implicitly

Asymptotic equation on the density

For low Stokes number, we obtain a diffusion equation on the number density

$$\frac{\partial \rho}{\partial t} + \frac{\partial \rho \bar{u}_g}{\partial x} = \frac{\partial}{\partial x} \left(St \lambda \frac{\partial \rho}{\partial x} \right)$$

The velocity and the internal energy are then written:

$$u = u_g - \frac{St \lambda}{\rho} \frac{\partial \rho}{\partial x}, \quad \varepsilon = \frac{St}{2} \left(\mu - \lambda \frac{\partial u}{\partial x} \right)$$

One may want to recover the asymptotic behavior - not natural for classical schemes

Asymptotic behavior / model coupling

In the zones of the flow where $\tau_g = 0$ and thus $\lambda = \mu = 0$, when no particle trajectory crossing is present, we should solve for

PGD system of equations

$$\frac{\partial \rho}{\partial t} + \frac{\partial \rho u}{\partial x} = 0$$

$$\frac{\partial \rho u}{\partial t} + \frac{\partial \rho u^2}{\partial x} = -\frac{\rho(u - \bar{u}_g)}{St}$$

Outline

- 1 High order moment methods in size, with realizable and accurate numerical methods
- 2 High order moment methods in velocity, with realizable and accurate numerical methods
 - Up to second order moment methods (statistical crossing)
 - Higher order moment methods (deterministic crossing)
 - Multi-Gaussian model
- 3 **Dealing with model coupling and asymptotic limits**
 - **A Hybrid model and related relaxation scheme**
 - An Asymptotic-Preserving Relaxation scheme

A relaxation scheme for PGD

Without the drag, the PGD system can be seen as the limit as $\eta \rightarrow +\infty$ of the system:

Relaxed Euler system of equations

$$\begin{aligned}\frac{\partial \rho}{\partial t} + \frac{\partial \rho u}{\partial x} &= 0 \\ \frac{\partial \rho u}{\partial t} + \frac{\partial \rho u^2 + P}{\partial x} &= -\frac{\rho(u - \bar{u}_g)}{St} \\ \frac{\partial \rho E}{\partial t} + \frac{\partial \rho E u + P u}{\partial x} &= -\frac{\rho u(u - \bar{u}_g)}{St} - \eta \rho \varepsilon\end{aligned}$$

and we solve the convective part of the pressure relaxation model taking $\eta = 0$

$$\begin{cases} \partial_t \rho + \partial_x(\rho u) = 0, \\ \partial_t(\rho u) + \partial_x(\rho u^2 + \Pi) = 0, \\ \partial_t(\rho E) + \partial_x(\rho E u + \Pi u) = 0, \\ \partial_t(\rho \Pi) + \partial_x(\rho \Pi u + a^2 u) = 0, \end{cases}$$

$$\partial_t \mathcal{V} + \partial_x \mathcal{G}(\mathcal{V}) = 0. \quad (5)$$

A relaxation scheme for PGD

We then solve

$$\begin{cases} \partial_t \rho = 0, \\ \partial_t(\rho u) = 0, \\ \partial_t(\rho E) = 0, \\ \partial_t(\rho \Pi) = \eta \rho(\rho - \Pi), \end{cases}$$

in the asymptotic regime $\eta \rightarrow \infty$. The conservative variables ρ , ρu and ρE are thus constant, while Π is set to be equal to ρ in this step.

A relaxation scheme for PGD

We now give the Riemann solution. We propose to take a nonconstant in the Riemann solution and we choose to solve

$$\partial_t a + u \partial_x a = 0. \quad (6)$$

The diagonal form is given by

$$\begin{cases} \partial_t(\Pi + au) + (u + a\tau)\partial_x(\Pi + au) = 0, \\ \partial_t(\Pi - au) + (u - a\tau)\partial_x(\Pi - au) = 0, \\ \partial_t(\Pi + a^2\tau) + u\partial_x(\Pi + a^2\tau) = 0, \\ \partial_t\left(\varepsilon - \frac{\Pi^2}{2a^2}\right) + u\partial_x\left(\varepsilon - \frac{\Pi^2}{2a^2}\right) = 0, \\ \partial_t a + u\partial_x a = 0. \end{cases}$$

The quantities $(\Pi \pm au)$, respectively $(\Pi + a^2\tau)$, $(\varepsilon - \frac{\Pi^2}{2a^2})$ and a , are (strong) Riemann invariants for the eigenvalues $u \pm a\tau$, resp. u .

A relaxation scheme for PGD

The self-similar Riemann solution $(x, t) \mapsto \mathcal{V}(x/t; \mathcal{V}_L, \mathcal{V}_R; a_L, a_R)$ and initial data

$$\mathcal{V}(x, t = 0) = \begin{cases} \mathcal{V}_L & \text{if } x < 0, \\ \mathcal{V}_R & \text{if } x > 0, \end{cases}$$

is made of four constant states $\mathcal{V}_L, \mathcal{V}_L^*, \mathcal{V}_R^*$ and \mathcal{V}_R , separated by three contact discontinuities associated with $\lambda_k = \lambda_k(\mathcal{V})$, $k = 1, 2, 3$ and propagating with speeds denoted by $\lambda(\mathcal{V}_L, \mathcal{V}_L^*)$, $\lambda(\mathcal{V}_L^*, \mathcal{V}_R^*)$ and $\lambda(\mathcal{V}_R^*, \mathcal{V}_R)$. More precisely, we have

$$\mathcal{V}\left(\frac{x}{t}; \mathcal{V}_L, \mathcal{V}_R\right) = \begin{cases} \mathcal{V}_L & \text{if } \frac{x}{t} < \lambda(\mathcal{V}_L, \mathcal{V}_L^*), \\ \mathcal{V}_L^* & \text{if } \lambda(\mathcal{V}_L, \mathcal{V}_L^*) < \frac{x}{t} < \lambda(\mathcal{V}_L^*, \mathcal{V}_R^*), \\ \mathcal{V}_R^* & \text{if } \lambda(\mathcal{V}_L^*, \mathcal{V}_R^*) < \frac{x}{t} < \lambda(\mathcal{V}_R^*, \mathcal{V}_R), \\ \mathcal{V}_R & \text{if } \lambda(\mathcal{V}_R^*, \mathcal{V}_R) < \frac{x}{t}. \end{cases}$$

A relaxation scheme for PGD

The intermediate states \mathcal{V}_L^* , \mathcal{V}_R^* , as well as the speeds of propagation, are determined and yield: $\lambda(\mathcal{V}_L, \mathcal{V}_L^*) = \lambda_1(\mathcal{V}_L) = u_L - a_L \tau_L$, $\lambda(\mathcal{V}_L^*, \mathcal{V}_R^*) = u^*$, $\lambda(\mathcal{V}_R^*, \mathcal{V}_R) = \lambda_3(\mathcal{V}_R) = u_R + a_R \tau_R$ and

$$u_L^* = u_R^* = u^* = \frac{a_L u_L + a_R u_R + \Pi_L - \Pi_R}{a_L + a_R},$$

$$\Pi_L^* = \Pi_R^* = \frac{a_R \Pi_L + a_L \Pi_R - a_L a_R (u_R - u_L)}{a_L + a_R},$$

$$\frac{1}{\rho_L^*} = \frac{1}{\rho_L} + \frac{a_R (u_R - u_L) + \Pi_L - \Pi_R}{a_L (a_L + a_R)}, \quad \frac{1}{\rho_R^*} = \frac{1}{\rho_R} + \frac{a_L (u_R - u_L) + \Pi_R - \Pi_L}{a_R (a_L + a_R)},$$

$$\varepsilon_L^* = \varepsilon_L - \frac{\Pi_L^2}{2a_L^2} + \frac{\Pi^{*2}}{2a_L^2}, \quad \varepsilon_R^* = \varepsilon_R - \frac{\Pi_R^2}{2a_R^2} + \frac{\Pi^{*2}}{2a_R^2}.$$

At this stage, the initial states \mathcal{V}_L and \mathcal{V}_R and more precisely the free parameters a_L and a_R are implicitly assumed to be such that the waves in the Riemann solutions are ordered as they should, namely

$$\lambda_1(\mathcal{V}_L) = u_L - \frac{a_L}{\rho_L} < u^* < \lambda_3(\mathcal{V}_R) = u_R + \frac{a_R}{\rho_R}. \quad (7)$$

A relaxation scheme for PGD

Following Bouchut (2004), we define $a_L = a_L(\mathcal{V}_L)$ and $a_R = a_R(\mathcal{V}_R)$ as follows:
 if $\rho_R \geq \rho_L$

$$\frac{a_L}{\rho_L} = \max(c_L, c_{min}) + \alpha \left(\frac{\rho_R - \rho_L}{\rho_R c_R} + u_L - u_R \right)_+,$$

$$\frac{a_R}{\rho_R} = \max(c_R, c_{min}) + \alpha \left(\frac{\rho_L - \rho_R}{a_L} + u_L - u_R \right)_+,$$

if $\rho_R \leq \rho_L$

$$\frac{a_R}{\rho_R} = \max(c_R, c_{min}) + \alpha \left(\frac{\rho_L - \rho_R}{\rho_L c_L} + u_L - u_R \right)_+,$$

$$\frac{a_L}{\rho_L} = \max(c_L, c_{min}) + \alpha \left(\frac{\rho_R - \rho_L}{a_R} + u_L - u_R \right)_+,$$

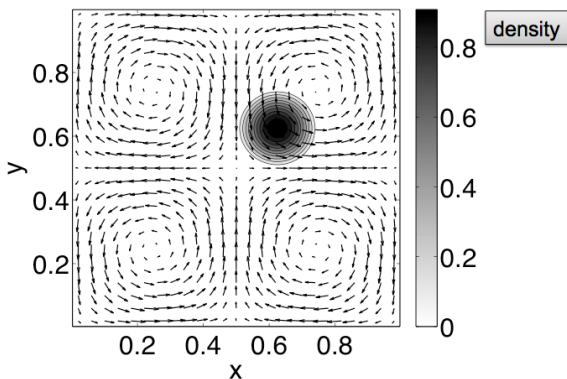
with $\alpha = (\gamma + 1)/2$, $c_{min} > 0$ and where $\rho_{L,R} = \rho_{L,R}(\mathcal{U}_{L,R})$, $c_{L,R} = c_{L,R}(\mathcal{U}_{L,R})$.

First, it is shown to fulfill (7) and to give the **positivity of the intermediate densities** ρ_L^* and ρ_R^* . Then, it complies with the **sub-characteristic condition** $a > \rho c$. At last, it guarantees the **nonlinear stability of the underlying relaxation scheme** that will be described in the following, and the **possibility of handling vacuum** in the sense that the speeds of propagation $\lambda_1(\mathcal{V}_L)$ and $\lambda_3(\mathcal{V}_R)$ remain finite. **Discrete entropy inequalities as well as maximum principles can be proved.**

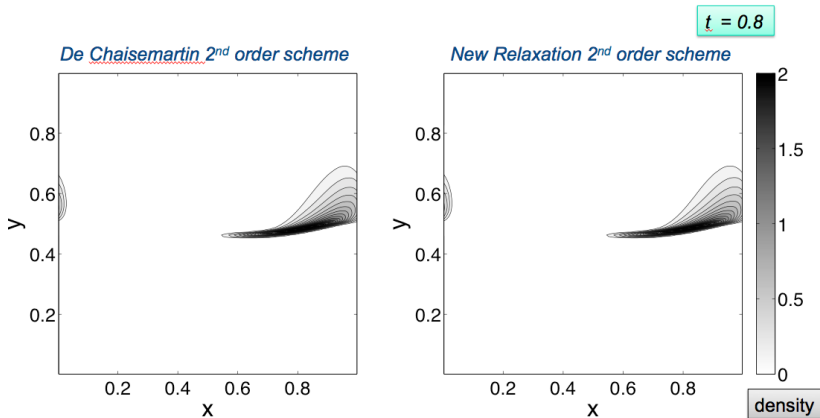
A relaxation scheme for PGD : Results

$t = 0$

Taylor-Green vortices of the gaseous flow and initial droplet distribution



A relaxation scheme for PGD : Results



A Hybrid model and related relaxation scheme

It is important to notice that the same formalism will be used for both systems. Just note that in the pressureless case, E must be understood as a function of the unknowns ρ and ρu , namely

$$E = \frac{(\rho u)^2}{2\rho},$$

but not as an unknown with evolution given by the passive transport equation

$$\partial_t \rho E + \partial_x (\rho E u) = 0.$$

We use a Godunov scheme for the first step before projection:

$$\mathcal{V}_j^{n+1-} = \mathcal{V}_j^n - \frac{\Delta t}{\Delta x} (g(\mathcal{V}_j^n, \mathcal{V}_{j+1}^n) - g(\mathcal{V}_{j-1}^n, \mathcal{V}_j^n)),$$

$$j \in \mathbb{Z}, \quad n \geq 0,$$

where the numerical flux function writes for all $j \in \mathbb{Z}$

$$g(\mathcal{V}_j^n, \mathcal{V}_{j+1}^n) = \mathcal{G}\left(\mathcal{V}(0; \mathcal{V}_j^n, \mathcal{V}_{j+1}^n; a_L(\mathcal{V}_j^n), a_R(\mathcal{V}_{j+1}^n))\right). \quad (8)$$

Let us recall that the numerical flux (8) is here explicitly known.

A Hybrid model and related relaxation scheme

We set for all $j \in \mathbb{Z}$

$$\mathcal{V}_j^{n+1} = \begin{pmatrix} \mathcal{U}_j^{n+1} \\ (\rho\Pi)_j^{n+1} \end{pmatrix} \quad (9)$$

with

$$\mathcal{U}_j^{n+1} = \mathcal{U}_j^{n+1-} \quad \text{and} \quad (\rho\Pi)_j^{n+1} = \rho(\mathcal{U}_j^{n+1})$$

in the case of the gas dynamics equations, and

$$\mathcal{U}_j^{n+1} = \left(\rho, \rho u, \frac{(\rho u)^2}{2\rho} \right)_j^{n+1-} \quad \text{and} \quad (\rho\Pi)_j^{n+1} = 0$$

in the pressureless case. This is equivalent to solve in the asymptotic regime

$\eta = +\infty$

$$\begin{cases} \partial_t \rho = 0, \\ \partial_t (\rho u) = 0, \\ \partial_t (\rho E) = 0, \\ \partial_t (\rho \Pi) = -\eta \rho (\rho - \Pi), \end{cases} \quad (10)$$

in the case of the gas dynamics equations, and for PGD:

$$\begin{cases} \partial_t \rho = 0, \\ \partial_t (\rho u) = 0, \\ \partial_t (\rho E) = -\eta \rho \varepsilon, \\ \partial_t (\rho \Pi) = -\eta \rho (\rho - \Pi), \end{cases} \quad (11)$$

A Hybrid model and related relaxation scheme

Recall that the conservative unknowns are ρ , ρu and ρE for the gas dynamics and ρ and ρu for the PGD. The main difference then clearly lies in **the treatment of the energy equation**.

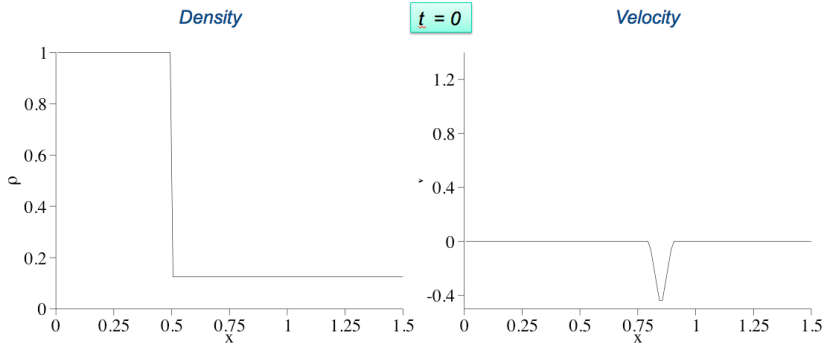
For the sake of clarity, we begin by introducing a color function Y such that $Y = 1$ for gas dynamics and $Y = 0$ for PGD. From a numerical point of view, a given cell C_j^n is said to be **pressureless**, $Y_j^n = 0$, if the internal energy $\varepsilon_j^n = (\rho E - \frac{(\rho u)^2}{2\rho})_j^n$ is **less than a given threshold ε_{min}** , and **with pressure**, $Y_j^n = 1$, otherwise.

In agreement with the threshold c_{min} already introduced for the sound speed in the definition of a_L and a_R , we set

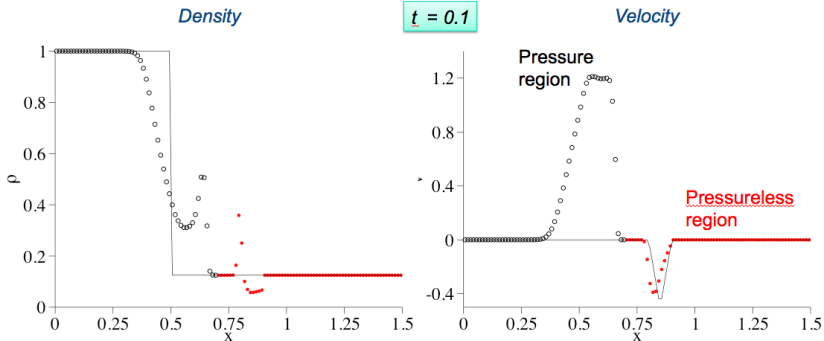
$$\varepsilon_{min} = \frac{c_{min}^2}{\gamma(\gamma - 1)}. \quad (12)$$

We thus distinguish between zones with PGD where the internal energy is exactly zero and zones where the energy level is above the defined small threshold, a property which is preserved by the pure convective part of the evolution.

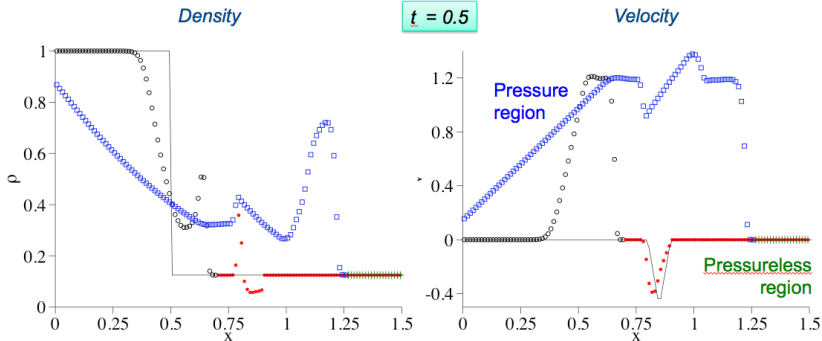
A Hybrid model and related relaxation scheme : Results



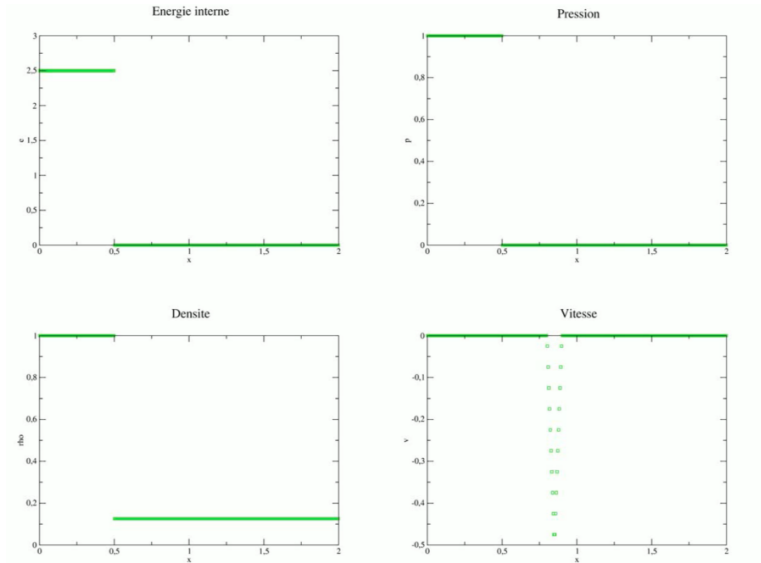
A Hybrid model and related relaxation scheme : Results



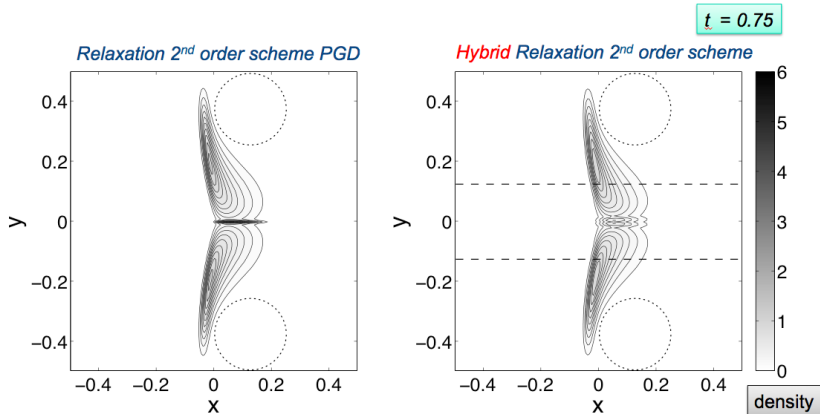
A Hybrid model and related relaxation scheme : Results



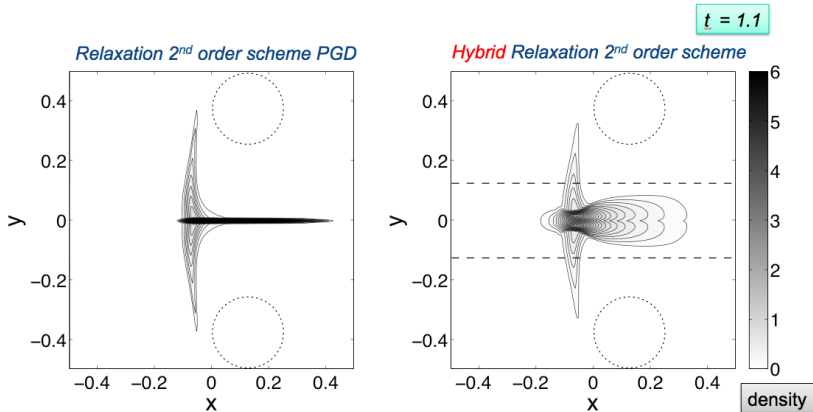
A Hybrid model and related relaxation scheme : Results



A Hybrid model and related relaxation scheme : Results



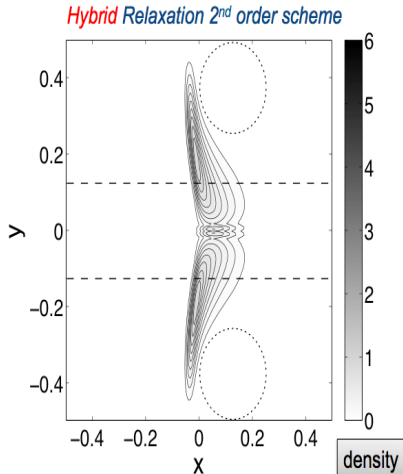
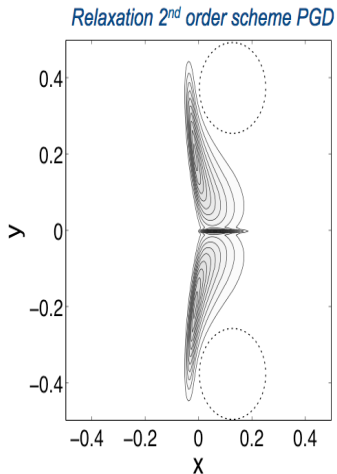
A Hybrid model and related relaxation scheme : Results



A Hybrid model and related relaxation scheme : Results

Pressureless gas dynamics: no subgrid energy source

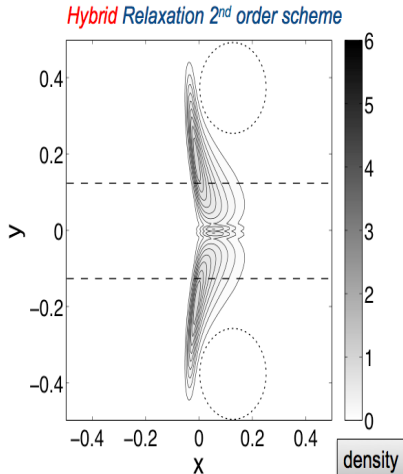
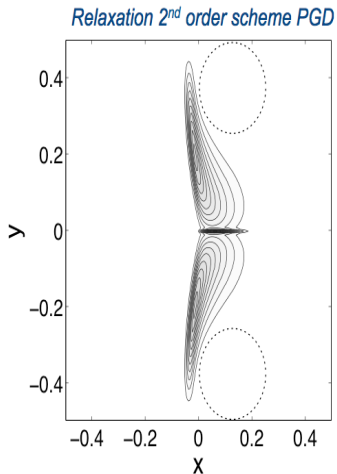
$t = 0.75$



A Hybrid model and related relaxation scheme : Results

Hybrid scheme: subgrid energy source in the center layer

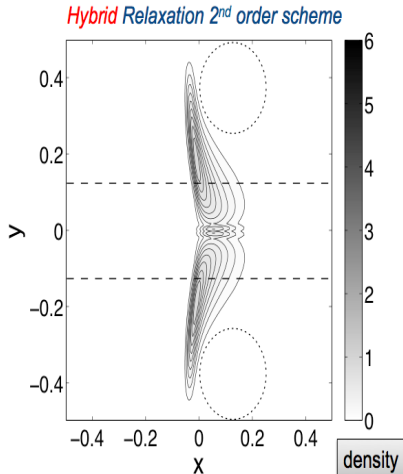
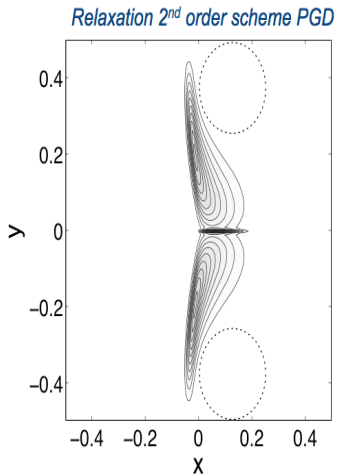
$t = 0.75$



A Hybrid model and related relaxation scheme : Results

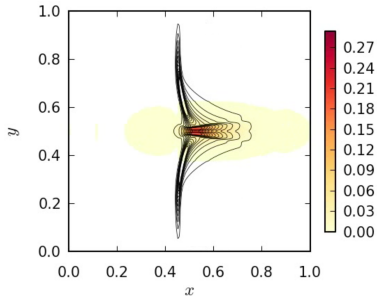
Hybrid scheme: subgrid energy source in the center layer

$t = 0.75$



A Hybrid model and related relaxation scheme

Hybrid scheme: original way of coupling pressureless and gas dynamics
(or high order KBMM - AG)
with accurate transport of number density and velocity



Boileau, Chalons, Massot, SIAM SISC, 2015 - HAL

Outline

- 1 High order moment methods in size, with realizable and accurate numerical methods
- 2 High order moment methods in velocity, with realizable and accurate numerical methods
 - Up to second order moment methods (statistical crossing)
 - Higher order moment methods (deterministic crossing)
 - Multi-Gaussian model
- 3 **Dealing with model coupling and asymptotic limits**
 - A Hybrid model and related relaxation scheme
 - **An Asymptotic-Preserving Relaxation scheme**

Gaussian closure and 3-equation system

Euler-like system of equations

$$\begin{aligned}\frac{\partial \rho}{\partial t} + \frac{\partial \rho u}{\partial x} &= 0 \\ \frac{\partial \rho u}{\partial t} + \frac{\partial \rho u^2 + P}{\partial x} &= -\frac{\rho(u - \bar{u}_g)}{St} \\ \frac{\partial \rho E}{\partial t} + \frac{\partial \rho u E + P}{\partial x} &= -\frac{\rho u(u - \bar{u}_g)}{St} - \frac{\rho(2\varepsilon - St\mu(St))}{St}\end{aligned}$$

where:

$$\rho = M^0, \quad \rho u = M^1, \quad \rho E = \frac{1}{2}M^2, \quad \rho\varepsilon = M^2 - M^0 u^2, \quad P = 2\rho\varepsilon + \rho\lambda(St)$$

The subgrid scale influence is seen on the source terms as well as on the pressure law

Asymptotic behavior

Considering the expression of λ and μ :

$$\lambda = \frac{\tau_g}{St(1 + St)}, \quad \mu = \frac{\tau_g}{St(1 + St)}$$

where τ_g is the subgrid scale energy of the gas phase.

Sound speed

The sound speed tends to infinity when St tends to 0:

$$c = \sqrt{6\varepsilon + 3\lambda} \xrightarrow[St \rightarrow 0]{} \infty$$

One may want to treat the acoustic part implicitly

Asymptotic equation on the density

For low Stokes number, we obtain a diffusion equation on the number density

$$\frac{\partial \rho}{\partial t} + \frac{\partial \rho \bar{u}_g}{\partial x} = \frac{\partial}{\partial x} \left(St \lambda \frac{\partial \rho}{\partial x} \right)$$

The velocity and the internal energy are then written:

$$u = u_g - \frac{St \lambda}{\rho} \frac{\partial \rho}{\partial x}, \quad \varepsilon = \frac{St}{2} \left(\mu - \lambda \frac{\partial u}{\partial x} \right)$$

One may want to recover the asymptotic behavior - not natural for classical schemes

An Asymptotic-Preserving Relaxation scheme

Main ingredients of the numerical scheme

Chalons, Girardin and Kokh, 2014 SISC

- **Lagrange-Projection** Coquel and al., 2010
- **Relaxation strategy** Chalons and Coquel, 2005
- **HLLC scheme with source terms** Gallice 2003, Chalons et al. 2010

Lagrange-Projection

Principles

Idea: Separate the acoustic waves from the transport velocity

Design principle: Splitting of the fluxes

Lagrangian step: implicit or explicit step

$$\frac{\partial \rho}{\partial t} + \rho \frac{\partial u}{\partial x} = 0$$

$$\frac{\partial \rho u}{\partial t} + \rho u \frac{\partial u}{\partial x} + \frac{\partial P}{\partial x} = -\frac{\rho(u - \bar{u}_g)}{St}$$

$$\frac{\partial \rho E}{\partial t} + \rho E \frac{\partial u}{\partial x} + \frac{\partial P u}{\partial x} = -\frac{\rho u(u - \bar{u}_g)}{St} - \frac{\rho(2\varepsilon - St\mu)}{St}$$

Transport step: explicit step

$$\frac{\partial \rho}{\partial t} + u \frac{\partial \rho}{\partial x} = 0$$

$$\frac{\partial \rho u}{\partial t} + u \frac{\partial \rho u}{\partial x} = 0$$

$$\frac{\partial \rho E}{\partial t} + u \frac{\partial \rho E}{\partial x} = 0$$

The lagrangian step is written in lagrangian coordinates $\tau = 1/\rho$ and $\tau \partial_x = \partial_m$

$$\frac{\partial \tau}{\partial t} - \frac{\partial u}{\partial m} = 0$$

$$\frac{\partial u}{\partial t} + \frac{\partial P}{\partial m} = -\frac{(u - \bar{u}_g)}{St}$$

$$\frac{\partial E}{\partial t} + \frac{\partial P u}{\partial m} = -\frac{u(u - \bar{u}_g)}{St} - \frac{(2\varepsilon - St\mu)}{St}$$

Relaxation strategy

Principles

Idea: Deal with a larger system but with a simpler structure, avoiding non-linearities

Design principle: Consider Π as a new unknown of the system that we denote Π

At the beginning of each time step, we impose that $\Pi = p$:

$$\frac{\partial \tau}{\partial t} - \frac{\partial u}{\partial m} = 0$$

$$\frac{\partial u}{\partial t} + \frac{\partial \Pi}{\partial m} = -\frac{(u - \bar{u}_g)}{St}$$

$$\frac{\partial E}{\partial t} + \frac{\partial \Pi u}{\partial m} = -\frac{u(u - \bar{u}_g)}{St} - \frac{(2\varepsilon - St\mu)}{St}$$

$$\frac{\partial \Pi}{\partial t} + a^2 \frac{\partial \Pi}{\partial m} = 0$$

where $a > \rho c$.

Adding the change of variable $w^\pm = \Pi \pm au$:

$$\frac{\partial \tau}{\partial t} - \frac{\partial u}{\partial m} = 0$$

$$\frac{\partial w^+}{\partial t} + a \frac{\partial w^+}{\partial m} = -\frac{(u - \bar{u}_g)}{St}$$

$$\frac{\partial w^-}{\partial t} - a \frac{\partial w^-}{\partial m} = \frac{(u - \bar{u}_g)}{St}$$

$$\frac{\partial E}{\partial t} + \frac{\partial \Pi u}{\partial m} = -\frac{u(u - \bar{u}_g)}{St} - \frac{(2\varepsilon - St\mu)}{St}$$

HLLC with source terms

Principles

Idea: Taking into account the source terms in the intermediate state of the HLLC scheme

Design principle: the source term is evaluated at the interfaces, instead of the cell centers

$$\partial_t \mathbf{U} + \partial_x \mathbf{F}(\mathbf{U}) = \mathbf{S}(\mathbf{U})$$

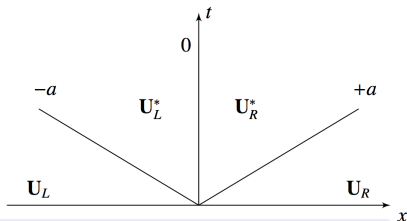
where:

$$\mathbf{U} = (\tau, \vec{w}, \overleftarrow{w}, E)^T, \quad \mathbf{F}(\mathbf{U}) = (u, a\vec{w}, -a\overleftarrow{w}, \Pi u)^T,$$
$$\mathbf{S}(\mathbf{U}) = \left(0, -\frac{u - \bar{u}_g}{St}, \frac{u - \bar{u}_g}{St}, -u \frac{u - \bar{u}_g}{St} - \frac{2\epsilon - St\mu}{St} \right)^T$$

HLLC scheme with source terms

Four-state approximation

$$\mathbf{W}\left(\frac{m}{t}; \mathbf{U}_L, \mathbf{U}_R\right) = \begin{cases} \mathbf{U}_L, & \frac{m}{t} < -a \\ \mathbf{U}_L^*, & -a < \frac{m}{t} < 0 \\ \mathbf{U}_R^*, & 0 < \frac{m}{t} < a \\ \mathbf{U}_R, & \frac{m}{t} > a \end{cases}$$



Consistency in the integral sense with source terms

$$\int_{-\Delta x/2}^{\Delta x/2} \mathbf{W}(x; \mathbf{U}_L, \mathbf{U}_R) dx = \frac{\Delta x}{2} (\mathbf{U}_L + \mathbf{U}_R) - \Delta t (\mathbf{F}_L + \mathbf{F}_R) + \Delta t \Delta x \tilde{\mathbf{S}}(\mathbf{U}_L, \mathbf{U}_R)$$

where:

$$\lim_{\substack{\mathbf{U}_L, \mathbf{U}_R \rightarrow \mathbf{U} \\ \Delta t, \Delta x \rightarrow 0}} \tilde{\mathbf{S}}(\Delta x, \Delta t; \mathbf{U}_L, \mathbf{U}_R) = \mathbf{S}(\mathbf{U})$$

Using Rankine-Hugoniot relationships, all the states are defined

Final scheme

$$\mathbf{U}_j^{n+1} = \mathbf{U}_j^n - \frac{\Delta t}{\Delta m_j} (\mathbf{F}_{j+1/2}^n - \mathbf{F}_{j-1/2}^n) + \frac{\Delta t}{2} \left(\frac{\Delta m_{j+1/2}}{\Delta m_j} \mathbf{S}_{j+1/2}^n + \frac{\Delta m_{j-1/2}}{\Delta m_j} \mathbf{S}_{j-1/2}^n \right) + \Delta t \mathbf{S}_j^{E-n}$$

where:

$$\mathbf{F}_{j+1/2}^n = \begin{pmatrix} u_{j+1/2}^* \\ a w_{j+1/2}^{+,*} \\ -a w_{j+1/2}^{-,*} \\ p_{j+1/2}^* u_{j+1/2}^* \end{pmatrix}, \quad \mathbf{S}_{j+1/2}^n = \begin{pmatrix} 0 \\ -\frac{a}{St} (u_{j+1/2}^* - \bar{u}_g) \\ \frac{a}{St} (u_{j+1/2}^* - \bar{u}_g) \\ -\frac{u_{j+1/2}^*}{St} (u_{j+1/2}^* - \bar{u}_g) \end{pmatrix}, \quad \mathbf{S}_j^{E-n} = \begin{pmatrix} 0 \\ 0 \\ 0 \\ \frac{1}{St} (2\epsilon_j^n - St\mu) \end{pmatrix}$$

$$u_{j+1/2}^* = \frac{1}{2a + \frac{\Delta m_{j+1/2}}{St}} \left(a(u_{j+1}^n + u_j^n) - (\Pi_{j+1}^n - \Pi_j^n) + \frac{\Delta m_{j+1/2}}{St} \bar{u}_g \right)$$

$$p_{j+1/2}^* = \frac{\Pi_{j+1}^n + \Pi_j^n}{2} - \frac{a(u_{j+1}^n - u_j^n)}{2}$$

Projection step

The last step of the scheme is the projection step, which corresponds to the evolution to material waves. This step is done in an explicit manner to keep accuracy. Considering $\mathbf{X} = (\rho, \rho u, \rho E)^T$, the projection step is:

$$\mathbf{x}_j^{n+1} = \mathbf{x}_j^n + \frac{\Delta t}{\Delta x} \left[u_{j-1/2}^{*,+} \mathbf{x}_{j-1}^n + \left[u_{j+1/2}^{*,-} - u_{j-1/2}^{*,+} \right] \mathbf{x}_j^n - u_{j+1/2}^{*,-} \mathbf{x}_{j+1}^n \right]$$

where $\alpha^\pm = (\alpha \pm |\alpha|)/2$.

Finally

We have

- A Lagrange-Projection scheme that allows to separate acoustic and material waves, and to apply an implicit treatment on acoustic waves and an explicit treatment on material waves (to keep a good precision)
- A relaxation scheme that simplify the structure of the hyperbolic system resulting from the Lagrange-Projection
- A HLLC scheme that account for source terms at the interfaces

It leads to an optimal scheme that takes the better of existing strategies to overcome the problem raised by the asymptotic limits of our modeling approach

Theorem

Under the CFL condition and with sufficiently large a , the implicit-explicit in time numerical scheme is well defined and satisfies the stability properties :

- It is a conservative scheme for the density, as well as for velocity and energy when the source terms are omitted;
- the density is positive for all times provided that the initial density is positive;
- the scheme is asymptotic preserving.

The test case

Dispersion of a droplet cloud in a turbulent gas field

Test case proposed in Hyland et al. 1999

- Exact analytical solutions of the dispersion of a Dirac δ -function in the phase space (both in space and velocity)
- 1D and 2D cases
- time-evolving coefficients

Here:

- 1D cases
- equilibrium coefficients (constant in time)

Physics of the test case

- The initial droplet cloud is spread by the subgrid-scale of the gas phase
- the density gradients generate droplet fluxes through λ , due to the correlations imposed by the turbulence
- μ tends to relax the particle energy towards the gas subgrid energy

The test case

Initial and Boundary conditions

- Gaussian spatial distribution:

$$\rho_0(x) = 1 + \exp\left(-\frac{x^2}{2(\sigma_x^0)^2}\right) \text{ where } \sigma_x^0 = 0.05$$

- Zero initial velocity or internal energy for the disperse phase: $u_0 = 0$ and $\varepsilon_0 = 0$
- No mean gas velocity but non-zero subgrid energy: $\bar{u}_g = 0$, $\tau_g = 0.1$
- Dirichlet Boundary condition:
 $\mathbf{U}(t, x = -2) = \mathbf{U}(t = 0, x = -2)$,
 $\mathbf{U}(t, x = 2) = \mathbf{U}(t = 0, x = 2)$

Numerical parameters

$$CFL = 0.5, \Delta t = \min(\Delta t_{conv}, St/2)$$

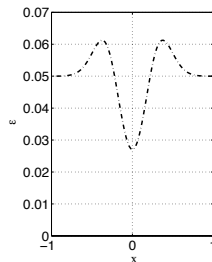
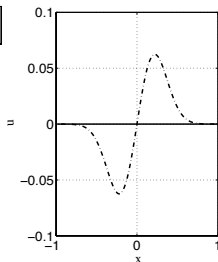
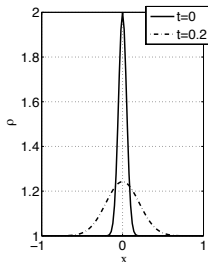
Analytical solution of the diffusion equation

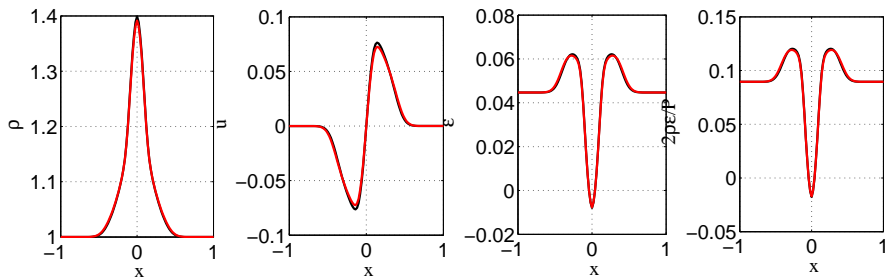
$$\rho(t, x) = 1 + \frac{\sigma_x^0}{\sigma_x(t)} \exp\left(-\frac{x^2}{2\sigma_x(t)^2}\right)$$

$$\sigma_x(t) = \sigma_x^0 + \sqrt{2\tau_g t}$$

$$u(t, x) = u_g - \frac{St\lambda}{\rho} \frac{\partial \rho(t, x)}{\partial x}$$

$$\varepsilon(t, x) = \frac{St}{2} \left(\mu - \lambda \frac{\partial u(t, x)}{\partial x} \right)$$

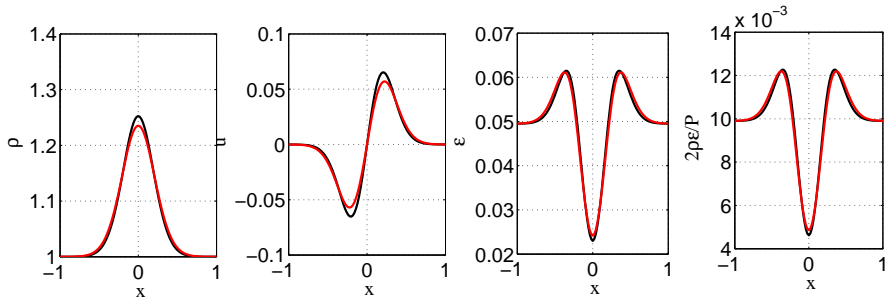


Effect of Stokes number: $N_{cell} = 100$, Stokes number = 10^{-1} 

black - AP scheme

red - non AP scheme

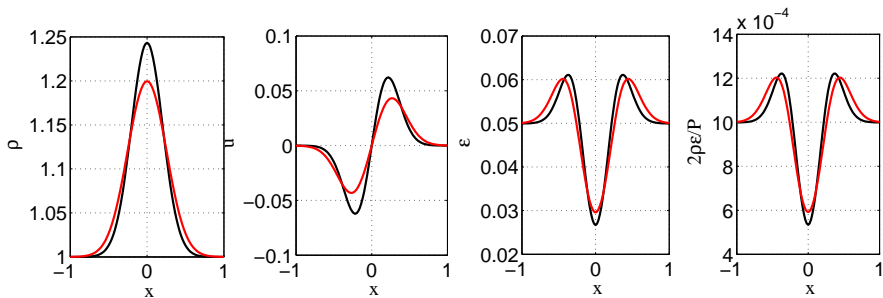
Effect of Stokes number: $N_{cell} = 100$, Stokes number = 10^{-2}



black - AP scheme

red - non AP scheme

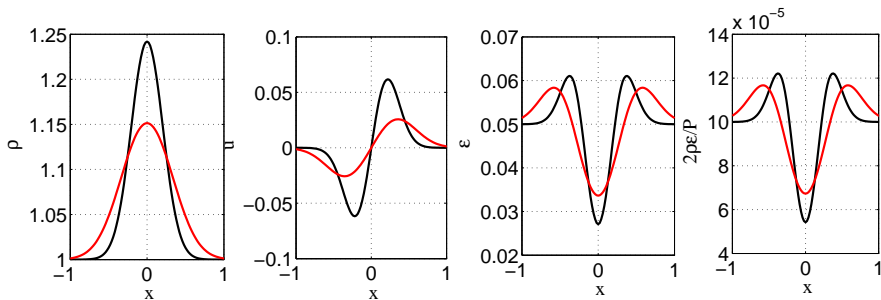
Effect of Stokes number: $N_{cell} = 100$, Stokes number = 10^{-3}



black - AP scheme

red - non AP scheme

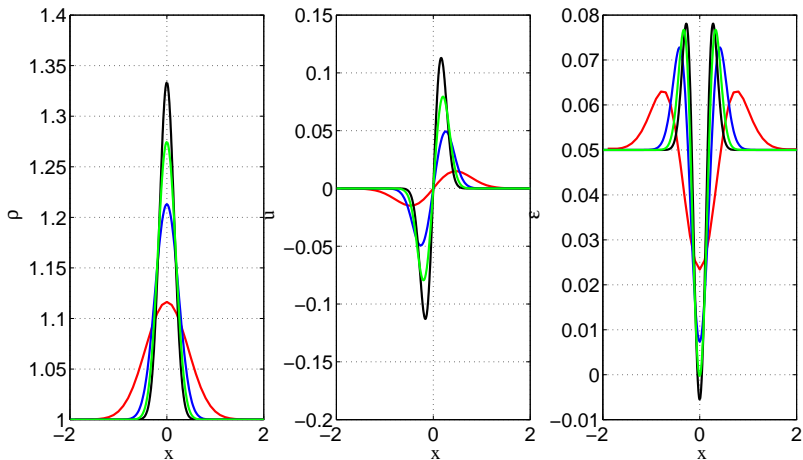
Effect of Stokes number: $N_{cell} = 100$, Stokes number = 10^{-4}



black - AP scheme

red - non AP scheme

Effect of discretization: Stokes number= 10^{-4} , non AP scheme



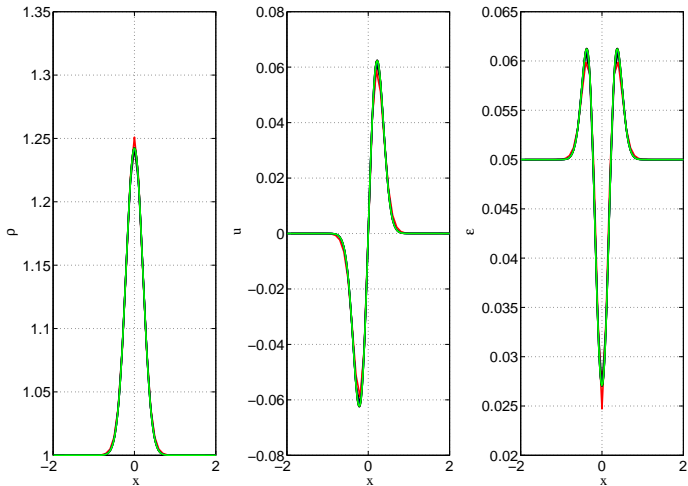
black - analytical

red - 40 cells

blue - 200 cells

green 600 cells

Effect of discretization: Stokes number= 10^{-4} , AP scheme



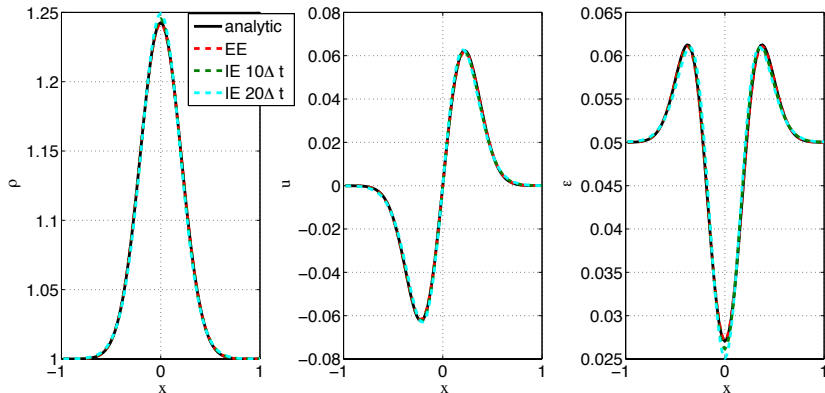
black - analytical

red - 40 cells

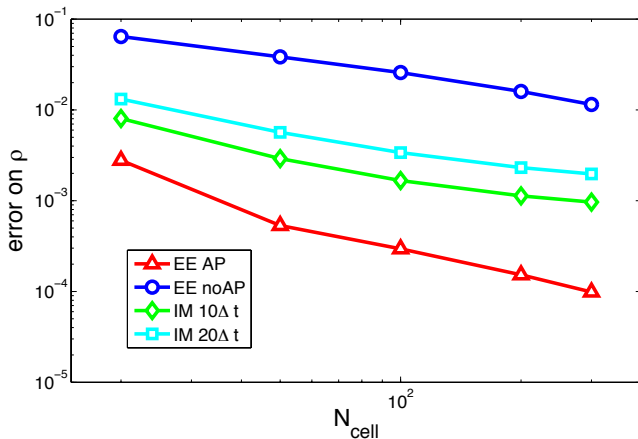
blue - 200 cells

green 600 cells

Implicit-Explicit formulation



Error on the density



While using a bigger time step, the Implicit-Explicit scheme gives really accurate results, where the non AP scheme needs a fine mesh to reach accurate results (Chalons, Massot, Vié - SIAM MMS 2015).

Conclusions

Conclusions - Coupling PGD/Euler

- A hybrid relaxation scheme has been derived, which can handle automatically the interface between the two models
- Second order in time and space can be achieved and PGD with accurate resolution can be used in zones where neither crossing nor subgrid agitation is to be found
- Can handle energy created by crossing

Conclusions - AP

- The AP Relaxation scheme of Chalons et al. have been extended to LES of disperse phase flows using the gaussian closure
- The results show the necessity of AP schemes, to keep a reasonable error regarding the asymptotic limit of the equations
- Moreover, the Implicit-Explicit formulation notably reduces the computational time, keeping the error an order of magnitude lower than a non AP scheme

Perspectives

Coupling of PGD with higher order velocity moment methods

- Anisotropic Gaussian (Cordier et al. 2014)

Extension of the AP scheme to systems adapted to higher Stokes number

- Higher order kinetic-based moment methods - Anisotropic Gaussian (Vié et al. 2015)
- Quadrature-based moment methods (Yuan and Fox, 2010, Kah et al 2010, Chalons et al 2012), Multi-Gaussian (Chalons et al. 2010, Vié et al 2014)

Extension to unstructured grids

- Convex-State-Preserving Discontinuous Galerkin methods applied to PGD and Euler-like equations (Larat et al. 2012, Sabat et al. 2014)
- How such an Asymptotic-Preserving strategy can be applied on unstructured grids?

Bibliography of the group



C. Chalons, R. O. Fox, F. Laurent, M. Massot, and A. Vié.

A multi-Gaussian quadrature-based moment method for dispersed multiphase flows.
[SIAM Journal on Multiscale Modeling and Simulation, in preparation, 2014.](#)



C. Chalons, R. O. Fox, and M. Massot.

A multi-Gaussian quadrature method of moments for gas-particle flows in a LES framework.
In [Proceedings of the Summer Program 2010, Center for Turbulence Research, Stanford University](#), pages 347–358, Stanford, 2010.



S. de Chaisemartin. [Eulerian models and numerical simulation of turbulent dispersion for polydisperse evaporating sprays.](#)

PhD thesis, Ecole Centrale Paris, France, 2009. Available online at <http://tel.archives-ouvertes.fr/tel-00443982/en/>.



F. Doisneau, F. Laurent, A. Murrone, J. Dupays, and M. Massot.

Eulerian multi-fluid models for the simulation of dynamics and coalescence of particles in solid propellant combustion.
[J. Comput. Phys.](#), 234:230–262, 2013.



D. Kah. [Taking into account polydispersity in the framework of a coupled Euler-Lagrange approach for the modeling of liquid fuel injection in internal combustion engines.](#)

PhD thesis, Ecole Centrale de Paris (2010) available online at <http://tel.archives-ouvertes.fr/tel-00618786/en/>.



D. Kah, F. Laurent, M. Massot, and S. Jay.

A high order moment method simulating evaporation and advection of a polydisperse spray.
[J. Comput. Phys.](#), 231(2):394–422, 2012.



A. Larat, A. Vié, and M. Massot.

A stable, robust and high order accurate numerical method for eulerian simulation of spray and particle transport on unstructured meshes.
[Annual Research Briefs of the CTR](#), pages 1–12, 2012.



M. Sabat, A. Larat, A. Vié, and M. Massot.

On the development of high order realizable schemes for the Eulerian simulation of disperse phase flows: a convex-state preserving Discontinuous Galerkin method.
[Journal of Comp. Physics](#) (2014) in preparation

Bibliography of the group



F. Laurent and M. Massot.

Multi-fluid modeling of laminar poly-dispersed spray flames: origin, assumptions and comparison of the sectional and sampling methods. [Combust. Theory and Modelling](#), 5:537–572, 2001.



F. Laurent, A. Vié, C. Chalons, R. O. Fox, and M. Massot.

A hierarchy of eulerian models for trajectory crossing in particle-laden turbulent flows over a wide range of stokes numbers. [Annual Research Briefs of the CTR](#), pages 1–12, 2012.



M. Massot, D. Kah, F. Laurent, and S. De Chaisemartin.

A robust moment method for the evaluation of the disappearance rate of evaporating sprays. [SIAM J. Appl. Math.](#), 70(8):3203–3234, 2010.



A. Vié, C. Chalons, R. O. Fox, F. Laurent, and M. Massot.

A multi-Gaussian quadrature method of moments for simulating high-Stokes-number turbulent two-phase flows. [Annual Research Briefs of the CTR](#), pages 309–320, 2011.



A. Vié, F. Doisneau and M. Massot.

On the Anisotropic Gaussian closure for the prediction of inertial-particle laden flows. [Comm. In Comput. Physics](#), 2015, 17 (1), pp.1-46



A. Vié, S. Jay, B. Cuenot, and M. Massot.

Accounting for polydispersion in the eulerian large eddy simulation of an aeronautical-type configuration. [Flow Turbulence and Combustion](#), Vol 90, 3 (2013) 545-581



A. Vié, F. Laurent, and M. Massot.

Size-velocity correlations in hybrid high order moment/multi-fluid methods for polydisperse evaporating sprays: modeling and numerical issues. [Journal of Computational Physics](#), Vol 237 (2013) 277-310

Bibliography of the group



A. Vié, E. Masi, O. Simonin and M. Massot.

On the Direct Numerical Simulation of moderate-Stokes-number turbulent particulate flows using Agebraic-Closure-Based and Kinetic-Based moment methods,

Volume «Summer Program 2012», publication of the Center for Turbulence Research, Stanford University (2012) 355-364



O. Emre, D. Kah, S. Jay, Q.H. Tran, A. Velghe, S. de Chaisemartin, R.O. Fox, F. Laurent, M. Massot,

Eulerian Moment Methods for Automotive Sprays,

(invited article) to a special issue of Atomization and Sprays (2014) 1-44



C. Chalons, M. Massot, A. Vié,

On the Eulerian Large Eddy Simulation of disperse phase flows: and asymptotic preserving scheme for small Stokes number flows,

in review, SIAM Multiscale Modeling and Simulation (2014) <http://hal.archives-ouvertes.fr/hal-00958108>



D. Kah, O. Emre, Q.H. Tran, S. de Chaisemartin, S. Jay, F. Laurent, and M. Massot,

High order moment method for polydisperse evaporating spray with mesh movement : application to internal combustion engines,

accepted in International Journal of Multiphase Flows (2014) <http://hal.archives-ouvertes.fr/hal-00941796>



M. Boileau, C. Chalons, M. Massot,

Robust numerical coupling of pressure and pressureless gas dynamics equations for Eulerian spray DNS and LES,

accepted in SIAM J. Sci. Comput. (2014) 1-22 <http://hal.archives-ouvertes.fr/hal-00906220>



O. Emre, R.O. Fox, M. Massot, S. de Chaisemartin, S. Jay, F. Laurent,

Eulerian modeling of a polydisperse evaporating spray under realistic internal-combustion-engine conditions,

in Press, Flow, Turbulence and Combustion, (2014) <http://hal.archives-ouvertes.fr/hal-00942115>



F. Doisneau, A. Sibra, J. Dupays, A. Murrone, F. Laurent, M. Massot,

An efficient and accurate numerical strategy for two-way coupling in unsteady polydisperse moderately dense sprays: application to Solid Rocket Motor instabilities,

Journal of Propulsion and Power, Vol 30, No. 3 (2014) 727-748 <http://hal.archives-ouvertes.fr/hal-00745991>

Bibliography of the group



C. Chalons, D. Kah, M. Massot,

Beyond pressureless gas dynamics : Quadrature-based velocity moment models,
[Communication in Mathematical Sciences](#), Vol. 10, Issue 4 (2012) 1241-1272



M. Sabat, A. Larat, A. Vié, M. Massot,

On the development of high order realizable schemes for the Eulerian simulation of disperse phase flows: a convex-state preserving Discontinuous Galerkin method,
selected from ICMF2013 in Press in [Journal of Computational Multiphase Flows](#) Vol 6, No. 3 (2014) 247–270



C. Yuan, F. Laurent and R.O. Fox,

An extended quadrature method of moments for population balance equations.
[Journal of Aerosol Science](#), 51(2012):1 – 23.



S. de Chaisemartin, L. Freret, D. Kah, F. Laurent, R.O. Fox, J. Reveillon and M. Massot,

Turbulent combustion of polydisperse evaporating sprays with droplet crossing: Eulerian modeling of collision at finite Knudsen and validation,
Volume du «Summer Program 2008», publication du Center for Turbulence Research de Stanford University (2009) 12 pages,
<http://www.stanford.edu/group/ctr/Summer/SP08/index.html>



F. Laurent, M. Massot, R. O. Fox,

Numerical simulation of polydisperse, dense liquid sprays in an Eulerian framework: direct quadrature method of moments and multi-fluid method,
[Journal of Computational Physics](#), Vol. 227, No. 6 (2008) 3058-3088 <http://hal.archives-ouvertes.fr/hal-00157269/fr/>



M. Massot, F. Laurent, S. de Chaisemartin, L. Fréret and D. Kah,

Eulerian multi-fluid models: modeling and numerical methods,
in "[Modelling and Computation of Nanoparticles in Fluid Flows](#)", NATO RTO AVT 169 Lectures of the von Karman Institute (2009) 86 pages - <http://hal.archives-ouvertes.fr/hal-00423031/fr/>



M. Massot, F. Laurent-Nègre, D. Kah, S. de Chaisemartin,

A robust moment method for the evaluation of the disappearance rate of evaporating sprays,
[SIAM Journal of Applied Maths](#), Vol. 70, No. 8 (2010) 3203-3234 <http://hal.archives-ouvertes.fr/hal-00332423/fr/>

Ph.D. Theses in the group



M. Sabat,

Eulerian models and dedicated numerical methods for polydisperse turbulent sprays
[Ph.D. Ecole Centrale Paris, 2015.](#)



A. Sibra,

Modeling and simulation of aluminum spray combustion in solid rocket propulsion using Eulerian multi-fluid methods
[Ph.D. Ecole Centrale Paris, Collaboration with ONERA, 2014.](#)



O. Emre,

Modeling and simulation of two-way coupling using high order moment methods in moderately dense polydisperse sprays occurring in internal combustion engines
[Ph.D. Ecole Centrale Paris, Collaboration with IFPE, 2014.](#)



F. Doisneau,

Modeling and simulation of polydisperse spray of alumina particles down to nanoparticles issued from the combustion of solid propellants in rocket engines
[Ph.D. Ecole Centrale Paris, Collaboration with ONERA, 2013. <https://tel.archives-ouvertes.fr/tel-01009896>](#)



D. Kah,

Modeling and simulation of polydispersity and two-way coupling using high order moment methods in moderately dense sprays occurring in internal combustion engines – <https://tel.archives-ouvertes.fr/tel-00618786>
[Ph.D. Ecole Centrale Paris, Collaboration with IFPE, 2010. SMAI \(France\) and ECCOMAS prizes \(Europe\) for best Ph.D.](#)



S. de Chaisemartin,

Modeling and simulation of turbulent dispersion of polydisperse sprays
[Ph.D. Ecole Centrale Paris, 2009. <https://tel.archives-ouvertes.fr/tel-00443982>](#)



G. Dufour,

Eulerian multi-fluid model for the description of sprays
[Ph.D. Université de Toulouse, Collaboration with ONERA, 2005.](#)



F. Laurent

Mathematical modeling and numerical simulation of polydisperse spray combustion
[Ph.D. Université de Lyon, 2002. <https://tel.archives-ouvertes.fr/tel-00185806>](#)

References of the talk



F.A. Williams,

Spray Combustion and Atomization
[Physics of Fluids](#) 1(1958):541–545



M. Boileau, S. Pascaud, E. Ribet, B. Cuenot, L.Y.M. Gicquel, T. Poinot, and M. Cazalens.

Investigation of two-fluid methods for Large Eddy Simulation of spray combustion in Gas Turbines.
[Flow, Turbulence and Combustion](#), 80(3):291–321, 2008.



F. Bouchut, S. Jin, and X. Li.

Numerical approximations of pressureless and isothermal gas dynamics.
[SIAM J. Numer. Anal.](#), 41(1):135–158, 2003.



C. Chalons, M. Girardin, and S. Kokh.

Large time step and asymptotic preserving numerical schemes for the gas dynamics equations with source terms.
[SIAM J. Sci. Comput.](#), 35(6): A2874-A2902, 2013.



P. Février, O. Simonin, and K. D. Squires.

Partitioning of particle velocities in gas-solid turbulent flow into a continuous field and a spatially uncorrelated random distribution: theoretical formalism and numerical study.
[J. Fluid Mech.](#), 533:1–46, 2005.



K.E. Hyland, S. McKee, and M. W. Reeks.

Exact analytic solutions to turbulent particle flow equations.
[Phys. Fluids](#), 11(5):1249–1261, 1999.



A. Kaufmann, M. Moreau, O. Simonin, and J. Helie.

Comparison between Lagrangian and mesoscopic Eulerian modelling approaches for inertial particles suspended in decaying isotropic turbulence.
[J. Comput. Phys.](#), 227:6448–6472, 2008.

References of the talk



E. Masi and O. Simonin.

An algebraic-closure-based moment method for unsteady Eulerian modeling of non-isothermal particle-laden turbulent flows in very dilute regime and high Stokes number.

[Turb. Heat and Mass Transf.](#), 7:1–12, 2012.



M. Moreau, B. Bédard, and O. Simonin.

Development of gas-particle euler-euler LES approach: a priori analysis of particle sub-grid models in homogeneous isotropic turbulence.

[Flow Turbulence and Combustion](#), 84(2):295–324, 2010.



M. W. Reeks.

On a kinetic equation for the transport of particles in turbulent flows.

[Phys. Fluids](#), 3:446–456, 1991.



C. Yuan and R.O. Fox.

Conditional quadrature method of moments for kinetic equations.

[J. Comput. Phys.](#), 230(22):8216–8246, 2011.



L.I. Zaichik, O. Simonin, and V.M. Alipchenkov.

An eulerian approach for large eddy simulation of particle transport in turbulent flows.

[Journal of Turbulence](#), 10(4):1–21, 2009.

References of the talk I



Bird, G. A. (1994).

Molecular gas dynamics and the direct simulation of gas flows.
[Oxford Science Publications](#), 42.



Bouchut, F. (1994).

On zero pressure gas dynamics.
In [Advances in kinetic theory and computing](#), pages 171–190. World Sci. Publishing, River Edge, NJ.



Bouchut, F., Jin, S., and Li, X. (2003).

Numerical approximations of pressureless and isothermal gas dynamics.
[SIAM J. Num. Anal.](#), 41:135–158.



Chalons, C., Fox, R. O., Laurent, F., Massot, M., and Vié, A. (2013).

A multi-Gaussian quadrature-based moment method for dispersed multiphase flows.
[SIAM Journal on Multiscale Modeling and Simulation](#), in preparation.



Chalons, C., Kah, D., and Massot, M. (2012).

Beyond pressureless gas dynamics: quadrature-based velocity moment models.
[Communication in Mathematical Sciences](#), 10(4):1241–1272.
Available online at <http://hal.archives-ouvertes.fr/hal-00535782/en>.



de Chaisemartin, S. (2009).

Eulerian models and numerical simulation of turbulent dispersion for polydisperse evaporation sprays.
PhD thesis, Ecole Centrale Paris, France.
Available on TEL : <http://tel.archives-ouvertes.fr/tel-00443982/en/>.



de Chaisemartin, S., Freret, L., Kah, D., Laurent, F., Fox, R. O., Reveillon, J., and Massot, M. (2009).

Eulerian models for turbulent spray combustion with polydispersity and droplet crossing : modeling and validation.
In [Proceedings of the Summer Program 2008, Center for Turbulence Research, Stanford University](#), pages 265–276.

References of the talk II



Dette, H. and Studden, W. J. (1997).

The theory of canonical moments with applications in statistics, probability, and analysis.

Wiley Series in Probability and Statistics: Applied Probability and Statistics. John Wiley & Sons Inc., New York.
A Wiley-Interscience Publication.



Doisneau, F. (2013).

Eulerian modeling and simulation of polydisperse moderately dense coalescing spray flows with nanometric-to-inertial droplets: application to Solid Rocket Motors.

PhD thesis, Ecole Centrale Paris, France.
Available on TEL : <http://tel.archives-ouvertes.fr/tel-01009896>.



Dufour, G. (2005).

Modélisation multi-fluide eulérienne pour les écoulements diphasiques à inclusions dispersées.

PhD thesis, Université Paul Sabatier Toulouse III.



Dukowicz, J. K. (1980).

A particle-fluid numerical model for liquid sprays.

J. Comput. Phys., 35(2):229–253.



Fox, R. O., Laurent, F., and Massot, M. (2008).

Numerical simulation of spray coalescence in an Eulerian framework: direct quadrature method of moments and multi-fluid method.

J. Comput. Phys., 227(6):3058–3088.



Freret, L., Lacour, C., de Chaisemartin, S., Laurent, F., Massot, M., Ducruix, S., and Durox, D. (2008).

Pulsated free jet with polydisperse spray injection, experiments and numerical simulation.

In Proceedings of the 32nd Symp. (International) on Combustion, The Comb. Institute, Montreal.



Fréret, L., Thomine, O., Réveillon, J., de Chaisemartin, S., Laurent, F., and Massot, M. (2010).

On the role of preferential segregation in flame dynamics in polydisperse evaporating sprays.

Proceedings of the Summer Program 2010. Center for Turbulence Research, Stanford.

References of the talk III



Laurent, F. (2006).

Numerical analysis of Eulerian multi-fluid models in the context of kinetic formulations for dilute evaporating sprays.
[M2AN Math. Model. Numer. Anal.](#), 40(3):431–468.



Laurent, F. and Massot, M. (2001).

Multi-fluid modeling of laminar poly-dispersed spray flames: origin, assumptions and comparison of the sectional and sampling methods.
[Comb. Theory and Modelling](#), 5:537–572.



Masi, E. and Simonin, O. (2012).

An algebraic-closure-based moment method for unsteady Eulerian modeling of non-isothermal particle-laden turbulent flows in very dilute regime and high Stokes number.
[Turb. Heat and Mass Transf.](#), 7:1–12.



Massot, M., Laurent, F., Kah, D., and de Chaisemartin, S. (2010).

A robust moment method for evaluation of the disappearance rate of evaporating sprays.
[SIAM J. Appl. Math.](#), 70(8):3203–3234.



Mead, L. R. and Papanicolaou, N. (1984).

Maximum entropy in the problem of moments.
[J. Math. Phys.](#), 25(8):2404–2417.



O'Rourke, P. (1981).

[Collective drop effects on vaporizing liquid sprays.](#)
PhD thesis, Los Alamos National Laboratory 87545, University of Princeton.



Simonin, O., Février, P., and Lavieville, J. (2002).

On the spatial distribution of heavy particle velocities in turbulent flow: from continuous field to particulate chaos.
[J. Turb.](#), 3(1):40.

References of the talk IV



Tagliani, A. (1999).

Hausdorff moment problem and maximum entropy: a unified approach.

[Appl. Math. Comput.](#), 105(2-3):291–305.



Yuan, C., Laurent, F., and Fox, R. O. (2012).

An extended quadrature method of moments for population balance equations.

[Journal of Aerosol Science](#), 51(0):1 – 23.

Acknowledgments

We gratefully acknowledge

- The support from the RTRA DIGITEO and ECP for the Post-doctoral fellowship for A.Vié. The present study received a funding from this RTRA through the MUSE project (PI M. Massot - "MULTIscale Spray combustion fully Eulerian solver in 3D : a new generation of numerical methods and algorithms, high performance simulations, validation and visualization").
- The support of Center for Turbulence Research for the Senior Fellowship (sabbatical) for M. Massot, as well as the support from ECP and the France-Stanford Center For Interdisciplinary Studies (2011-2012 grant for P. Moin / M. Massot).
- The support of the Center for Turbulence Research and the France-Stanford collaborative project (PI P. Moin and M. Massot) for the visit of A. Vié and C. Chalons at Stanford.

THANK YOU FOR YOUR ATTENTION